Title: The Major Facilitator Superfamily Transporter ZIFL2 Modulates Cesium And Potassium Homeostasis In *Arabidopsis*

Running head: *Arabidopsis ZIFL2 mediates Cs^+ and K^+ homeostasis*

Corresponding author: Dr. P. Duque; Instituto Gulbenkian de Ciência, Rua da Quinta Grande, 6, 2780-156 Oeiras, Portugal, Tel.: (351) 214464630; Fax: (351) 214407970; E-mail: duquep@igc.gulbenkian.pt

The Major Facilitator Superfamily transporter ZIFL2 modulates cesium and potassium homeostasis in *Arabidopsis*

Running head: Arabidopsis ZIFL2 mediates Cs^+ and K^+ homeostasis

Estelle Remy[1], Tânia R. Cabrito[2], Rita A. Batista[1], Miguel C. Teixeira[2], Isabel Sá-Correia[2] and Paula Duque[1]

[1] Instituto Gulbenkian de Ciência, 2780-156 Oeiras, Portugal

[2] Institute for Biotechnology and BioEngineering (IBB), Center for Biological and Chemical Engineering, Department of Bioengineering, Instituto Superior Técnico, University of Lisbon, 1049-001 Lisbon, Portugal

Abbreviations: β-glucuronidase (GUS); Columbia ecotype (Col-0); green fluorescent protein (GFP); Major Facilitator Superfamily (MFS); Murashige and Skoog medium (MS medium); reverse transcription-PCR (RT-PCR); Transfer DNA (T-DNA); untranslated region (UTR); yellow fluorescent protein (YFP).

Abstract

Potassium (K^+) is an essential mineral nutrient for plant growth and development, with numerous membrane transporters and channels having been implicated in the maintenance and regulation of its homeostasis. The cation cesium (Cs^+) is toxic for plants but shares similar chemical properties to the K^+ ion and hence competes with its transport. Here, we report that K^+ and Cs^+ homeostasis in *Arabidopsis thaliana* also requires the action of ZIFL2 (Zinc-Induced Facilitator-Like 2), a member of the Major Facilitator Superfamily (MFS) of membrane transporters. We show that the *Arabidopsis* ZIFL2 is a functional transporter able to mediate K^+ and Cs^+ influx when heterologously expressed in yeast. Promoter-reporter, RT-PCR and fluorescent protein fusion experiments indicate that the predominant ZIFL2.1 isoform is targeted to the plasma-membrane of endodermal and pericyle root cells. *ZIFL2* loss of function and overexpression respectively exacerbate and alleviate plant sensitivity upon Cs^+ and excess K^+ supply, also influencing Cs^+ whole-plant partitioning. We propose that the activity of this *Arabidopsis* MFS carrier promotes cellular K^+ efflux in the root, thereby restricting Cs^+/K^+ xylem loading and subsequent root-to-shoot translocation under conditions of Cs^+ or high K^+ external supply.

Keywords: *Arabidopsis thaliana*; heterologous expression; MFS transporter; potassium and cesium homeostasis; root; *Saccharomyces cerevisiae*.

Introduction

In plants, potassium (K^+) is a macronutrient essential for optimal growth and development. In fact, it represents the most abundant inorganic cation in these organisms, comprising up to 10% of their dry weight (Leigh and Jones 1984). Involved in enzyme activation, protein charge neutralization and maintenance of the photosynthetic apparatus, K^+ plays a key role in cellular metabolism (Marschner 2012). Owing to its high mobility, K^+ also acts as a major osmoticum driving plant movements, such as tropisms or stomatal opening/closure, and promoting shoot cellular expansion and axial growth, but also regulates membrane potential and cytoplasmic pH homeostasis (Maathuis 2009). Last but not least, K^+ serves as a mobile energy source for photosynthate translocation through the phloem (Gajdanowicz et al. 2011) as well as a major signaling component mediating plant stress responses (Amtmann et al. 2008).

K^+ is primarily acquired from the soil as a monovalent cation that, once absorbed into the root epidermis, moves both apoplastically and symplastically through the adjacent cell layers to reach the stele. After secretion into the stellar apoplast and subsequent loading into the xylem vessels for translocation to the shoot via root pressure and the transpiration stream, K^+ is delivered to the leaf apoplastic space outside the bundle sheath. It is then transferred to the phloem sap before allocation to aerial sink organs or recycling back to the root, the amount of recirculated K^+ ultimately tuning up K^+ root absorption and xylem loading. Besides cell-to-cell movements, intracellular K^+ homeostasis also relies largely on vacuolar partitioning (recently reviewed in Ahmad and Maathuis 2014).

All steps in plant K^+ homeostasis, from initial root acquisition to subsequent distribution among different tissues and subcellular trafficking, require the concerted action of multiple K^+ membrane transport systems. Such carriers, either secondary active transporters or channels, have been primarily characterized in *Arabidopsis thaliana* and belong to nine major families (reviewed in Aleman et al. 2011; Anschutz et al. 2014; Sharma et al. 2013; Szczerba et al. 2009): (i) Shaker-type K^+ channels (nine members); (ii) Tandem-pore K^+ channels (TPK; six members); (iii) Cation/H^+ antiporters (CPA) subfamily 1 or Na^+/H^+ exchangers (NHX; six members); (iv) CPA subfamily 2 or Cation/H^+ exchangers (CHX; 28 members); (v) K^+ uptake permeases/High-affinity K^+ transporters/K^+ transporters (KUP/HAK/KT; 13 members); (vi) High-affinity K^+ transporter (HKT; 1 member); (vii) K^+

efflux antiporters (KEA; six members); (viii) Cyclic-nucleotide-gated channels (CNGC; 20 members); (ix) Glutamate receptors (GLR; 20 members).

Although numerous of the above carriers indeed exhibit K^+ transport activity, relatively few have been assigned *in planta* functions. As expected, K^+ transporters/channels are primarily involved in K^+ cellular homeostasis and whole-plant distribution, mediating K^+ uptake under both K^+-replete and K^+ starvation conditions (HAK5 and AKT1, Gierth et al. 2005; Hirsch et al. 1998; Nieves-Cordones et al. 2010; Pyo et al. 2010; Qi et al. 2008; Rubio et al. 2008; CHX17, Cellier et al. 2004; CHX13, Zhao et al. 2008; GCNG10, Borsics et al. 2007), K^+ vacuolar partitioning (TPK1, Gobert et al. 2007; NHX1 and NHX2, Barragan et al. 2012; Bassil et al. 2011; NHX3, Liu et al. 2010), K^+ xylem loading (SKOR, Gaymard et al. 1998) or regulation of K^+ nutrient status (HKT1, Rus et al. 2004). On the other hand, K^+ transport activity of many carriers has been diverted to ensure such fundamental processes as guard cell osmoregulation (GORK, Hosy et al. 2003; KUP6/KUP8, Osakabe et al. 2013; CHX20, Padmanaban et al. 2007; TPK1, Gobert et al. 2007; KAT1, Kwak et al. 2001), response to water stress (AKT1, Nieves-Cordones et al. 2012), salt stress tolerance (GCNG10, Guo et al. 2008), reproduction (SKIP, Mouline et al. 2002; CHX21 and CHX23, Evans et al. 2012; Lu et al. 2011; TPK4, Becker et al. 2004), germination (CNGC3, Gobert et al. 2006), sugar loading into the phloem (AKT2/3, Deeken et al. 2002), energy generation (AKT2, Gajdanowicz et al. 2011), cellular expansion (KUP2, Elumalai et al. 2002; AKT1, Desbrosses et al. 2003), and polar transport of the phytohormone auxin (TRH1, Rigas et al. 2001; Vicente-Agullo et al. 2004).

We recently reported the functional characterization of a novel transporter from the Major Facilitator Superfamily (MFS), Zinc-Induced Facilitator-Like 1 (ZIFL1), which exhibits H^+-coupled K^+ transport activity (Remy et al. 2013b), pointing to a previously unrecognized role for this superfamily in K^+ transport. Interestingly, our work revealed that alternative splicing of the corresponding gene determines a dual function for this carrier – the full-length ZIFL1.1 protein is a root tonoplast-localized transporter involved in shootward auxin transport, while the truncated ZIFL1.3 splice form is targeted to the plasma membrane of guard cells where it regulates stomatal closure and hence plant drought tolerance (Remy et al. 2013b). By contrast, one of the two closest ZIFL1 homologs in *Arabidopsis*, ZIF1 (Zinc-Induced Facilitator 1), was described as a tonoplast-localized transporter promoting zinc

(Zn) tolerance by affecting vacuolar partitioning of nicotianamine, a low molecular mass chelator with high affinity for a range of transition metals (Haydon and Cobbett 2007; Haydon et al. 2012).

In the present study, we investigated the *in vivo* roles of the second closest homolog of the ZIFL1 transporter in *Arabidopsis*, ZIFL2. By combining functional analyses in *A. thaliana* and heterologous expression in *Saccharomyces cerevisiae*, we provide evidence that unlike ZIF1 and ZIFL1 this carrier plays a role in both K^+ and cesium (Cs^+) homeostasis.

Results

The predominant ZIFL2 transcript is ubiquitously expressed in Arabidopsis

According to the current genome annotation (TAIR10, www.arabidopsis.org), the *Arabidopsis ZIFL2* gene (At3g43790) contains 18 exons (Fig. 1A) and generates three distinct transcripts (Fig. 1B). The *ZIFL2.1* (At3g43790.1) and *ZIFL2.2* (At3g43790.2) transcripts are identical except for the presence of a 18-nt long stretch at the end of the sixteenth exon in *ZIFL2.2*, while the *ZIFL2.2* and *ZIFL2.3* (At3g43790.3) splice variants share an identical coding sequence and differ solely in their 3' untranslated region (UTR). According to bioinformatics software predictions (TMHMM Server v2, www.cbs.dtu.dk/services/TMHMM-2.0; Krogh et al. 2001), the three *ZIFL2* transcripts encode full-size carriers displaying the typical MFS transporter signature motif that includes two transmembrane domains, each consisting of six membrane-spanning segments, delimiting a central hydrophilic loop.

To initiate the characterization of the *ZIFL2* gene, we examined its tissue- and organ-specific expression patterns by reverse transcription-PCR (RT-PCR). As shown in Figure 1C, *ZIFL2* transcript levels were globally low but the gene was ubiquitously expressed throughout plant development, albeit to a lesser extent at early development stages. Importantly, in all tissues analyzed, the *ZIFL2.1* transcript made the primary contribution to total *ZIFL2* expression, in particular in seedlings and roots, while expression of the alternative *ZIFL2.2* and *ZIFL2.3* transcripts was barely detectable. This indicated that the two alternative splicing events are not favored under optimal growth conditions.

We next monitored the *ZIFL2* organ- and tissue-specific expression patterns by means of reporter gene experiments. Following staining of transgenic lines stably expressing a green fluorescent protein – β-glucuronidase (GFP-GUS) fusion under the control of the native *ZIFL2* promoter, homogenous GUS coloration restricted to the endodermal and pericycle cell layers was observed from the

hypocotyl-root junction throughout the primary root (Fig. 1D). Despite various attempts, we were unable to detect any staining in either lateral roots or other plant tissues, namely flowers and mature green organs – stems, leaves and siliques. In addition, *ZIFL2* promoter activity was insufficient to allow detection of the GFP signal in any of the tissues tested, including roots. Taken together, these results indicated that the ZIFL2 transporter, albeit generally lowly expressed, may exert a prominent role in roots.

The Arabidopsis ZIFL2 transporter is targeted to the plasma membrane

To determine the subcellular localization of the ZIFL2 transporter, we generated C-terminal yellow fluorescent protein (YFP) or GFP fusions with the ZIFL2.1 isoform under the control of the 35S promoter. Confocal microscopy analysis of the YFP signal upon transient expression in *Arabidopsis* protoplasts suggested that the carrier localizes to the plasma membrane (Fig. 2A, B). In order to further ascertain the site of action of ZIFL2, we performed co-localization experiments in tobacco leaf epidermal cells using specific tonoplast and plasma-membrane mCherry markers (Nelson et al. 2007). As seen in Figure 2C-Q, the ZIFL2.1-GFP fusion protein co-localized exclusively with the plasma membrane marker, whereas it did not match the distribution of the tonoplast marker, confirming that the ZIFL2 transporter is targeted to the plasma membrane of plant cells.

The ZIFL2 carrier catalyzes proton-coupled potassium transport activity

The identification of the physiological substrate(s) of a membrane transporter is of prime importance in dissecting the precise molecular mechanisms underlying its function. In a first attempt to identify the substrate(s) of the ZIFL2 carrier, we explored its transport properties by means of heterologous expression in *S. cerevisiae*. Correct expression of the GFP-ZIFL2.1 fusion protein in the *Δtpo1* deletion mutant, which lacks the MFS carrier Transporter of Polyamines 1 (Tpo1) conferring yeast resistance to a wide range of ionic and chemical stresses (*Saccharomyces* genome database, www.yeastgenome.org; do Valle Matta et al. 2001), was confirmed by immunoblotting (Fig. 3A). Subcellular localization studies further suggested that the plant transporter is targeted to the yeast plasma membrane (Fig. 3A), in agreement with the localization observed *in planta* (see Fig. 2). As shown in Fig. 3B, and in striking similarity with ZIFL1 (Remy et al. 2013b), expression of the ZIFL2 transporter confers slightly enhanced yeast resistance to two weak acids, malate and acetate, as well as to the metal ion thallium (Tl^{3+}), while dramatically reducing and increasing sensitivity to the metal

ions aluminum (Al^{3+}) and Cs^+, respectively. However, and in contrast to ZIFL1, ZIFL2 was unable to modulate yeast auxin sensitivity (data not shown).

Cs^+ ions share physicochemical properties with K^+ ions, rendering them potent inhibitors of at least some of the plant K^+ transport systems (Hampton et al. 2004; White and Broadley 2000; Zhu and Smolders 2000). We therefore decided to investigate whether the ZIFL2 transporter can also influence K^+ delivery to the yeast cell, by evaluating its capacity to rescue the deficient growth under limiting K^+ supply of the *Δqdr2* deletion mutant, which lacks the MFS transporter Quinidine Resistance 2 (Qdr2) (Vargas et al. 2007). As shown in Figure 3C, expression of the GFP-ZIFL2.1 fusion protein was able to markedly alleviate the pronounced growth defect induced by loss of Qdr2 at low K^+ concentrations to the same extent as the ZIFL1.1 transporter, strongly suggesting that the *Arabidopsis* ZIFL2 carrier also possesses K^+ transport activity.

As MFS transporters are single-polypeptide secondary carriers capable only of transporting small solutes in response to chemiosmotic ion gradients, catalyzing uniport, symport or antiport activities (Pao et al. 1998), we also analyzed the proton-dependence of ZIFL2 activity in yeast. In *S. cerevisiae*, intracellular pH regulation is essentially sustained by the action of the plasma membrane H^+-ATPase Pma1 (Serrano 1978). The activity of this proton pump and the passive proton influx through the yeast plasma membrane can be estimated by monitoring the pH of the external medium, so we compared the acidification curves of *Δqdr2* cells expressing the ZIFL2 or ZIFL1 transporters under growth-limiting K^+ conditions. Low K^+ levels were previously shown to lead to a reduced rate of extracellular medium acidification by yeast cells lacking Qdr2 when compared to the wild-type strain (Vargas et al. 2007). Figure 3D shows that expression of the GFP-ZIFL2.1 and GFP-ZIFL1.1 fusion proteins significantly and similarly increased the rate of H^+ efflux in *Δqdr2* mutant cells grown in medium with low K^+, demonstrating that, at least in yeast, the two *Arabidopsis* transporters share H^+-coupled K^+ transport activity.

Loss of ZIFL2 function affects potassium and cesium sensitivity in Arabidopsis

To gain insight into the *in vivo* function(s) of the ZIFL2 transporter, we isolated one mutant allele (SALK_059052) carrying a Transfer DNA (T-DNA) insertion in the *ZIFL2* gene and designated *zifl2-1* in accordance to Haydon and Cobbett (2007). Sequence analysis of the genomic DNA/T-DNA junctions determined that the insertion is located in the tenth exon of *ZIFL2* (see Fig. 1A). RT-PCR

142 analysis of *ZIFL2* expression in *zifl2-1* homozygous seedlings using primers annealing upstream of the
143 insertion site revealed transcript levels comparable to wild-type plants, but no expression was detected
144 when primers flanking or annealing downstream of the T-DNA segment were used (Fig. 4A). Thus, the
145 mutant allele produces a truncated *ZIFL2* transcript that lacks the sequence encoding most of the
146 central loop along with the entire second transmembrane domain and is thus unlikely to encode a
147 functional membrane transporter (Shin et al. 2004). This strongly suggested that *zifl2-1* is a true loss-
148 of-function mutant.

149 We then carried out a detailed phenotypical analysis of the *zifl2-1* mutant. When grown *in vitro*
150 under optimal conditions (~20 mM K^+), *zifl2-1* mutant seedlings appeared morphologically
151 indistinguishable from the corresponding wild type (Columbia ecotype; Col-0), showing normal shoot
152 growth, chlorophyll content and primary root elongation (Table 1). Unlike the *zifl1-2* mutant, which is
153 defective in lateral root system development and drought stress tolerance (Remy et al. 2013b), *zifl2-1*
154 exhibits normal lateral root emergence and elongation (Table 1) and transpiration rates
155 (Supplementary Fig. S1A). Moreover, the sensitivity of the *zifl2-1* mutant was unaltered upon extended
156 challenge with exogenous auxins (Supplementary Fig. S1B, Table 2) or in the presence of excessive
157 amounts of Zn (Supplementary Fig. S2, Table 2) in clear contrast to the *zifl1-2* or *zif1-2* mutants,
158 respectively (Haydon and Cobbett 2007; Remy et al. 2013b).

159 Prompted by the ZIFL2 heterologous expression results obtained in yeast (see Fig. 3) and given
160 the Cs^+ resistance phenotype previously observed in the *zifl1* mutant background (Remy et al. 2013b),
161 we next sought to evaluate the response of *zifl2-1* mutant seedlings to Cs^+ toxicity. In the presence of
162 excessive Cs^+ amounts, *Arabidopsis* seedlings develop toxicity symptoms, typically including shoot
163 growth retardation, leaf chlorosis and inhibition of primary root elongation (Hampton et al. 2004; Kanter
164 et al. 2010; Fig. 4B, C). Following exposure to a wide Cs^+ toxicity range, the inhibitory effect that this
165 ion exerts on primary root elongation was substantially attenuated in the *zifl2-1* mutant (Fig. 4B, C), to
166 a much greater extent than in the z*ifl1-2* mutant (Table 2; Remy et al. 2013b). Remarkably, the two
167 other Cs^+ toxicity hallmarks, shoot growth retardation and chlorosis, were visibly exacerbated in *zifl2-1*
168 when compared to the wild type (Fig. 4B, C). The non-essential heavy metal Cs has been observed to
169 severely inhibit K^+ assimilation, so that Cs^+ stress, along with the effects of its own toxicity, is
170 perceived by plant root cells as a K^+ deficiency (Hampton et al. 2004; White and Broadley 2000; Zhu

and Smolders 2000). As no significant differences in primary root elongation were observed between *zifl2-1* and wild-type seedlings under conditions of K^+ deficiency, even when assayed on media with global low cation content (Supplementary Fig. S3), we also examined the response of *zifl2-1* mutant seedlings to excess K^+ (Fig. 4B, C). As expected, a moderate increase in environmental K^+ availability improves photosynthesis rates, which in turn allows more effective shoot biomass production, while concomitantly restraining primary root elongation. However, when provided at very high levels, K^+ becomes deleterious to global plant growth (Hampton et al. 2004; Liu and Zhu 1997; Sahr et al. 2005). Noticeably, *zifl2-1* roots displayed significantly improved tolerance to inhibitory K^+ concentrations, while the mutant behaved as the wild type regarding shoot growth and chlorophyll content over a range of elevated K^+ supplies (Fig. 4B, C). As expected from publicly available microarray data (http://www.genevestigator.com; Zimmermann et al., 2004), we found that *ZIFL2* expression was unresponsive to exogenous Cs^+ or high K^+ in *Arabidopsis* roots (Supplementary Fig. S4). Collectively, these results indicated that the ZIFL2 carrier might play a role in Cs^+ and K^+ homeostasis in plant root cells.

The Arabidopsis ZIF1, ZIFL1 and ZIFL2 transporters are not functionally redundant

To further investigate the physiological roles of the ZIFL2 transporter and address the possibility of functional redundancy between the *Arabidopsis* *ZIF1*, *ZIFL1* and *ZIFL2* genes, we phenotypically compared the corresponding single mutants, along with the *zif1-2 zifl2-1* (Haydon and Cobbett 2007) and *zifl1-2 zifl2-1* (this study) double mutants. Because *ZIF1* (At5g13740) and *ZIFL1* (At5g13750) are tandem genes, obtaining the respective double mutant by regular crosses is likely improbable, as already noted by Haydon and Cobbett (2007).

None of the three single or two double mutants displayed significant differences from the wild type at the level of shoot growth, chlorophyll content or primary root elongation rate under control conditions (Table 1). As expected, lateral root development was similarly affected in the *zifl1-2* and *zifl1-2 zifl2-1* mutants, whereas it remained unaltered in all other mutant backgrounds. Similarly, reduced tolerance to Zn toxicity was restricted to the *zif1-2* and *zif1-2 zifl2-1* mutants, while sensitivity to exogenous auxins and resistance to high K^+ were confined to the *zifl1-2/zifl1-2 zifl2-1* mutants and *zifl2-1/zifl1-2 zifl2-1* mutants, respectively (Table 2). Moreover, the Cs^+ resistance phenotype displayed by the *zifl2-1* mutant, also detected in the *zifl1-2* mutant background albeit to a lesser extent, was not further

exacerbated in the *zifl1-2 zifl2-1* double mutant background. In agreement with previous findings (Haydon and Cobbett 2007; Remy et al. 2013a), these results strongly suggest that the ZIF1, ZIFL1 and ZIFL2 carriers do not fulfill overlapping functions and act in distinct physiological or metabolic processes.

ZIFL2 overexpression in Arabidopsis confers opposite phenotypes to zifl2-1 upon cesium and potassium challenges

To obtain further clues on the physiological relevance of the ZIFL2 transporter in Cs^+ and K^+ homeostasis, we selected two transgenic lines expressing the *ZIFL2.1-GFP* cDNA under the control of the 35S promoter in the wild-type background (*ZIFL2.1*OX1 and *ZIFL2.1*OX2). In order to exclude the possibility that the observed *zifl2-1* mutant phenotype results from disruption of another gene, we also selected two such lines after transformation of the *zifl2-1* mutant (*zifl2-1*/*ZIFL2.1*OX1 and *zifl2-1*/*ZIFL2.1*OX2). All these transgenic lines similarly displayed a significant increase in *ZIFL2* expression levels when compared to the wild type (Fig. 5A), with no obvious phenotypical alterations being detected between wild-type and *ZIFL2.1*-overexpressing seedlings under optimal growth conditions (Table 1). However, *ZIFL2.1* overexpression visibly exacerbated the detrimental effects of excessive Cs^+ on primary root elongation over a broad range of Cs^+ supplies, while substantially attenuating them at the level of both shoot growth and chlorophyll content (Fig. 5B, C). As for elevated K^+ supplies, *ZIFL2.1* overexpression also conferred significantly enhanced sensitivity to the transgenic roots, but development of the shoot and its chlorophyll content remained unaffected (Fig. 5B, C). Therefore, the Cs^+- and K^+-related phenotypes of *ZIFL2.1*-overexpressing lines were strikingly opposite to those displayed by the *zifl2-1* loss-of-function mutant, confirming the implication of ZIFL2 transport activity in plant Cs^+ and K^+ homeostasis.

Activity of the Arabidopsis ZIFL2 carrier affects cesium whole-plant partitioning

As an initial step towards unraveling the mechanisms by which the ZIFL2 transporter influences Cs^+ and K^+ homeostasis in *Arabidopsis*, we determined the Cs and K concentrations in shoot tissues from seedlings grown under control conditions (~20 mM K^+) or in the presence of moderate Cs^+ (2 mM) or K^+ (60 mM) stress (Fig. 6). As previously reported (Adams et al. 2013; Hampton et al. 2004), seedlings challenged with Cs^+ accumulated a non negligible amount of Cs in their above-ground parts (Fig. 6A), which concomitantly accumulated significantly less K when compared to their Cs-free counterparts

229 (Fig. 6B). Importantly, Cs^+-treated *zifl2-1* mutant and *ZIFL2.1*-overexpressing shoots concentrated on
230 average 30% more and 20% less Cs than wild-type shoots, respectively (Fig. 6A). By contrast, their
231 shoot K concentration was reduced to the same extent as in the wild type (Fig. 6B). Similarly, and
232 despite that as expected shoot K accumulation increased with the external K^+ concentration (Hampton
233 et al. 2004; Kanter et al. 2010), the shoot K concentration quantified in seedlings challenged with high
234 K^+ was globally comparable in all genotypes (Fig. 6B). These results are in clear agreement with the
235 gathered physiological data (see Figs. 4 and 5) and strongly suggest that ZIFL2 transport activity
236 influences Cs^+ but not K^+ whole-plant partitioning.

237 **Discussion**

238 Since the identification of AKT1 and KAT1, two members of the *Arabidopsis* Shaker-like channel
239 family, as the two first plant K^+ channels (Anderson et al. 1992; Sentenac et al. 1992), several carriers
240 from well-established channel or transporter families have been linked to plant K^+ homeostasis and to
241 a lesser extent also to Cs^+ homeostasis. To the best of our knowledge, the present study is the first to
242 functionally implicate an MFS transporter in such fundamental physiological processes, further hinting
243 at a broader role for this class of transporters in plant heavy-metal and ion homeostasis. Indeed, the
244 few plant MFS carriers functionally characterized so far are mainly involved in sugar (Buttner 2007),
245 nitrate/oligopeptide (Tsay et al. 2007) and phosphate (Nussaume et al. 2011) transport, while only two,
246 ZIF1 (Haydon and Cobbett 2007) and more recently ZIF2 (Remy et al. 2014), have been shown to
247 contribute to *Arabidopsis* Zn tolerance.

248 Several lines of evidence indicate that indeed the *Arabidopsis* ZIFL2 transporter plays a significant
249 role in K^+ and Cs^+ homeostasis. First, our heterologous expression studies show that ZIFL2 is able to
250 mediate K^+ influx into yeast cells without requiring additional plant-specific factors. Potassium transport
251 activity of most *Arabidopsis* carriers has been demonstrated through functional complementation of
252 yeast mutant strains defective in K^+ uptake, including Shaker-like (Anderson et al. 1992; Becker et al.
253 1996), TPK (Becker et al. 2004) and CNGC (Ali et al. 2006; Gobert et al. 2006; Kohler et al. 1999)
254 channels or CHX (Chanroj et al. 2011; Evans et al. 2012; Maresova and Sychrova 2006; Padmanaban
255 et al. 2007; Quintero and Blatt 1997; Zhao et al. 2008) and HAK/KT/KUP (Ahn et al. 2004; Fu and
256 Luan 1998; Kim et al. 1998; Rigas et al. 2001; Rubio et al. 2000) transporters. Furthermore, our yeast

experiments show that ZIFL2-mediated K^+ transport activity is proton coupled, in agreement with its classification as a member of the MFS that groups proton motive force-driven secondary carriers (Pao et al. 1998). Besides K^+ channels, which facilitate K^+ passive diffusion across membranes down its concentration gradient, all the K^+ carriers characterized to date mediate active K^+ transport coupled to the passive diffusion of protons down their electrochemical transmembrane gradient, generated primarily by either plasma membrane H^+-ATPases or vacuolar H^+-pyrophosphatases. While K^+ transporters from the HAK/KUP/KT and HKT/TRK families are K^+/H^+ symporters, those from the CHX, NHX and KEA families catalyze K^+/H^+ antiport activities (Ashley et al. 2006), as ZIFL2 appears to. Importantly, ZIFL2 activity also markedly exacerbates yeast sensitivity to Cs^+, consistent with this ion representing a competitive or opportunistic substrate of some plant K^+ transport systems, such as the high-affinity K^+ transporters HAK5 (Qi et al. 2008; Rubio et al. 2000), KAT1 (Schachtman et al. 1992) and KUP9 (Kobayashi et al. 2010). It should be noted that the effect of ZIFL2 expression is not restricted to K^+ and Cs^+, influencing also yeast responses to two weak acids (malate and acetate) and toxic ions (Al^{3+} and Tl^{3+}). Hence, and except for auxins, ZIFL2 and its closest homolog ZIFL1 share the exact same transport properties at least when expressed in yeast (Remy et al. 2013b), suggesting that their distinct *in planta* roles stem primarily from their different subcellular and tissue distribution.

A second line of evidence corroborating a role for the ZIFL2 transporter in plant Cs^+ homeostasis comes from our functional analysis of *ZIFL2* loss-of-function and *ZIFL2.1* overexpression lines. In agreement with our physiological data — i.e. *ZIFL2* loss-of-function and *ZIFL2.1* overexpression respectively enhancing and reducing Cs^+ sensitivity at the level of shoot biomass production and chlorophyll content —, shoots of *zifl2-1* mutant and *ZIFL2.1*-overexpressing seedlings exposed to Cs^+ stress accumulate significantly more and less Cs, respectively, than those from the wild type. Importantly, reduced shoot K concentration of the mutant and transgenic lines following Cs^+ exposure was not further affected as compared to the wild type. This indicates that the phenotypical alterations induced by *ZIFL2* loss-of-function and *ZIFL2.1* overexpression in *Arabidopsis* above-ground tissues are most likely linked to Cs^+ toxicity itself rather than to a concomitant change in K^+ supply, in agreement with Cs^+ toxicity not being solely perceived as K^+ starvation (Hampton et al. 2004; White and Broadley 2000; Zhu and Smolders 2000) and with the fact that we did not observe a *zifl2-1* phenotype under K^+ deficiency. Remarkably, the opposite trend was detected in root tissues, which

286 exhibit exacerbated tolerance and sensitivity to the inhibitory effect that Cs^+ exerts on primary root
287 elongation in the *zifl2-1* and *ZIFL2.1*-overexpression backgrounds, respectively. Together these
288 findings indicate that ZIFL2 function influences Cs^+ whole-plant partitioning. Cs^+ ions are believed to
289 be acquired at the root-soil interface through the K^+ uptake systems, before they move symplastically
290 until the xylem and translocate to the plant aerial tissues (Hampton et al. 2004; White and Broadley
291 2000). Uptake of K^+ ions by *Arabidopsis* root cells is chiefly dominated by activity of the AKT1 channel
292 and the HAK5 transporter (Gierth et al. 2005; Pyo et al. 2010; Rubio et al. 2008). While AKT1 does not
293 significantly contribute to root Cs^+ influx (Broadley et al. 2001), the HAK5 transporter mediates
294 substantial uptake and accumulation of this ion upon K^+ starvation (Qi et al. 2008), hitherto
295 representing the only carrier functionally implicated in Cs^+ homeostasis in *Arabidopsis*. Interestingly,
296 we recently reported that ZIFL1.1 activity negatively regulates Cs^+ tolerance at the level of primary root
297 inhibition, while excess Cs^+ suppresses lateral root emergence and elongation defects induced by both
298 *ZIFL1* loss-of-function and *ZIFL1.1* overexpression (Remy et al. 2013b). Nevertheless, because the
299 corresponding single mutations do not have additive or synergistic effects, the ZIFL2 and ZIFL1.1
300 transporters are unlikely to be functionally redundant in Cs^+ homeostasis.

301 In plants, Cs^+ ions are not relevant for any cellular or physiological process and therefore most
302 likely constitute an opportunistic rather than the natural substrate of the ZIFL2 transporter. In support
303 of this notion, our plant functional data also point to a role for the ZIFL2 carrier in K^+ homeostasis.
304 Primary root tolerance to adverse effects induced by a very high external K^+ supply is negatively
305 affected by ZIFL2 transport activity, in a similar trend as for Cs^+. Nonetheless, unlike with Cs^+, ZIFL2
306 activity appears insufficient to engender long-distance K^+ transport alterations. We propose that this is
307 due to the essential nature of K^+, for which plants have developed a very tightly controlled homeostatic
308 network aimed primarily at ensuring an adequate K^+ supply while preventing its toxic build-up at both
309 the whole-plant and cellular levels. This network is likely to involve at least partially functionally
310 redundant K^+ carriers, whose activity most certainly compensates for altered ZIFL2 levels.

311 Our transient expression assays in isolated *Arabidopsis* protoplasts indicate that, in contrast to its
312 ZIF1 and ZIFL1 homologs but in agreement with bioinformatics predictions (WoLF PSORT,
313 http://wolfpsort.seq.cbrc.jp), the ZIFL2 transporter is targeted to the plasma membrane of plant cells.
314 Unfortunately, we were unable to visualize any GFP signal in transgenic roots expressing ZIFL2.1-

GFP, despite detailed analysis of a large number of independent transformants. Nevertheless, the GFP-tagged ZIFL2.1 isoform was functionally active, as its overexpression was able not only to rescue the defects but also to induce exact opposite phenotypes to those observed in the *zifl2-1* mutant. The failure to detect the GFP signal *in planta* could be due to the orientation of the ZIFL2 transporter in the plasma membrane, i.e. N- and C-terminal extremities facing the acidic apoplasm, as both the absorbance and the fluorescence of the GFP protein are greatly sensitive to low pH (Kneen et al. 1998; Ward 1982).

Considering also the preferential expression of the ZIFL2 transporter in endodermal and pericycle cells of the mature root zone, the *zifl2-1* phenotype is consistent with ZIFL2 activity promoting (i) Cs^+/K^+ retention in the root, thereby restricting Cs^+/K^+ xylem loading and subsequent root-to-shoot translocation; or (ii) Cs^+/K^+ xylem retrieval, as hypothesized for the Na^+/K^+ channel CNGC10 whose loss of function results in the same whole-plant partitioning trend as the *zifl2-1* mutation except that for Na^+ instead of Cs^+ ions (Guo et al. 2008). However, the H^+-coupled K^+ transport activity of the ZIFL2 carrier is incompatible with it promoting cellular K^+ influx from the acidic xylem sap, while in agreement with it driving active cellular K^+ efflux to the apoplastic space under conditions of high external K^+ supply. Being an essential ion, the cytosolic concentrations of K^+ need to be maintained within narrow limits regardless of external K^+ abundance. Besides K^+ import/export at the tonoplast, intracellular K^+ homeostasis is tightly controlled via the integrated regulation of K^+ influx and efflux at the plasma membrane (White and Karley 2010). To date, two root plasma-membrane K^+ channels have been shown to mediate K^+ efflux in *Arabidopsis*: GORK in root hairs (Ivashikina et al. 2001) and SKOR in the stele (Gaymard et al. 1998). Though likely also controlled by other channels, K^+ loading into the xylem is largely sustained by the activity of SKOR, whose deletion triggers a significant reduction in shoot K accumulation due to lower K^+ delivery to the xylem sap (Gaymard et al. 1998). We propose that under Cs^+/K^+ excess, ZIFL2 efflux activity counteracts Cs^+/K^+ entry into the xylem by releasing it into the surrounding apoplasm of the endodermis and pericycle, thus preventing too much Cs^+/K^+ from reaching the shoot. We have recently shown that alternative splicing dictates a dual function for the ZIFL2 closest homolog, ZIFL1 (Remy et al. 2013b), and plays a key role in regulating the activity of the ZIF2 transporter (Remy et al. 2014). Functional and molecular characterization of the *ZIFL2.2* and

ZIFL2.3 splice variants should uncover the full extent of ZIFL2's role in the regulation of plant Cs^+/K^+ homeostasis.

Material and methods

Plant materials and growth conditions

The *A. thaliana* ecotype Col-0 was used in this study. T-DNA insertion mutants *zif1-2* (SALK_011408), *zifl1-2* (GABI_052H08) and *zifl2-1* (SALK_059052) were obtained from the Nottingham Arabidopsis Stock Centre (Nottingham, UK). The exact T-DNA insertion site in the *zifl2-1* mutant was confirmed using primers annealing at the T-DNA borders and gene-specific primers (Supplementary Table S1), which also allowed PCR-based genotyping to identify homozygous lines. The *zif1-2 zifl2-1* double mutant (Haydon and Cobbett 2007) was kindly provided by Scott Sinclair (Ruhr University Bochum, Germany), and the *zifl1-2 zifl2-1* double mutant was generated through genetic crossing of the two single mutant lines. Plant transformation was achieved by the floral-dip method (Clough and Bent 1998) using *Agrobacterium tumefaciens* strain EHA105.

Seeds were surface-sterilized and sown on Murashige and Skoog (1962) medium (MS medium) supplemented with 0.1 g l^{-1} *myo*-inositol and 0.5 g l^{-1} MES, adjusted to pH 5.7 and solidified with 0.8% phyto agar (Duchefa Biochemie B.V., Haarlem, The Netherlands). After 3 d of stratification, seeds were placed in a growth chamber and seedlings transferred to soil after 2-3 weeks. Plants were cultivated under long-day conditions (16-h light, 22°C/8-h dark, 18°C; 60% relative humidity).

Gene expression analyses

Total RNA was extracted from seedlings or tissues harvested from 8-wk old plants using TRIzol® reagent (Invitrogen, Life Technologies, Carlsbad, CA, USA) or the innuPREP Plant RNA kit (Analytik Jena, Jena, Germany) according to the manufacturers' instructions. RNA samples were treated with DNAse I (Promega, Madison, WI, USA) and phenol-chloroform purified before reverse transcription using M-MLV reverse transcriptase (Promega) following the protocol provided. First-strand cDNA was used as a template for semi-quantitative PCR amplification with primers designed to detect *ZIFL2, CYCLOPHILIN* (*ROC1)* and *UBIQUITIN10* (*UBQ10)* expression (Supplementary Table S1).

For native *ZIFL2* promoter reporter gene experiments, a fragment encompassing the 2383 bp immediately upstream of the start codon was PCR-amplified (Supplementary Table S1) from genomic

DNA and inserted via the *Sac*I/*Sac*II restriction sites into the pKGWFS7 plasmid containing a GFP-GUS fusion (Karimi et al. 2002). After introduction of the corresponding *ProZIFL2:GFP-GUS* construct into wild-type plants, two independent transformants showing similar tissue-specific GUS expression patterns were selected. Histochemical staining of GUS activity was performed as described by Sundaresan et al. (1995).

Generation of ZIFL2-overexpressing lines and subcellular localization studies

To generate ZIFL2.1 protein fusions with the YFP and GFP reporters, the *ZIFL2.1* transcript (5'UTR plus the coding sequence except the stop codon) was PCR-amplified (Supplementary Table S1), using root cDNA as a template, and inserted under the control of the 35S promoter into the YFP- or GFP-tagged versions of the pBA002 vector via the *Xho*I/*Pac*I restriction sites. Two transgenic lines displaying significant *ZIFL2.1* overexpression were recovered upon transformation of either wild-type or *zifl2-1* mutant plants with the resulting Pro*35S*:*ZIFL2.1-YFP* construct. This construct was also transfected by polyethylene glycol transformation (Abel and Theologis 1994) into *Arabidopsis* protoplasts generated as described by Yoo et al. (2007). Transient co-expression of the Pro*35S:ZIFL2.1-GFP* construct with the tonoplast marker γ-Tonoplast Intrinsic Protein (TIP)-mCherry or the plasma membrane marker Plasma membrane Intrinsic Protein 2A (PIP2A)-mCherry (Nelson et al. 2007) and the pBIN-NA construct (Silhavy et al. 2002) in leaf abaxial epidermal cells of *Nicotiana tabacum* was performed via the agroinfiltration procedure described by Voinnet et al. (2003) using *A. tumefaciens* strain GV3101.

Yeast manipulations

The *S. cerevisiae* deletion mutant strains BY4741_*Δtpo1* (*MATa, his3Δ1, leu2Δ0, met15Δ0, ura3Δ0, YLL028w::kanMX4*) and BY4741_*Δqdr2* (*MATa, his3Δ1, leu2Δ0, met15Δ0, ura3Δ0, YIL121W::kanMX4*) were used in this study. The *Arabidopsis ZIFL2.1* coding sequence was cloned into the *pGREG576* vector (Jansen et al. 2005), and expression of the corresponding GFP fusion protein was verified by western blotting and fluorescence microscopy as described in Cabrito et al. (2009). Strains and vector were acquired from the Euroscarf collection (Frankfurt, Germany). Susceptibility of the *Δtpo1* mutant to chemical stresses was assessed by spot assays carried out as previously described (Cabrito et al. 2009) in minimal MMB-U agarized medium supplemented with $Al_2(SO_4)_3$, $TlCl_3$, L-malic acid, acetic acid or CsCl at the specified concentrations (pH was adjusted to 4

for the weak acids). Growth of the *Δqdr2* mutant under K^+ limitation was evaluated by spot assays on agarized ammonium phosphate basal medium (KNA) supplemented with 0.2 or 2 mM KCl as previously described (Vargas et al. 2007). The *in vivo* active proton export of the *Δqdr2* mutant was evaluated by monitoring the external medium pH as in Vargas et al. (2007) using liquid KNA medium supplemented with 0.5 mM of KCl.

Phenotypical assays

All assays were performed in a climate-controlled growth cabinet under long-day conditions. After 5 d of vertically-oriented growth on control medium (~20 mM K^+), seedlings were transferred to fresh medium containing the indicated compound (Sigma-Aldrich, Saint-Louis, PO, USA) at the specified concentrations, with Zn^{2+}, Cs^+ and K^+ ions provided as $ZnCl_2$, CsCl or KCl. Primary root elongation and lateral root parameters, i.e. density and total length, were measured on scanned images using the ImageJ software (http://rsbweb.nih.gov/ij) after an additional 8 and 14 d of growth, respectively. Shoot biomass along with chlorophyll content were determined (Fankhauser and Casal 2004) after an additional two weeks of growth. Water loss and hypocotyl elongation assays were performed as described previously (Remy et al. 2013b).

Microscopy

Differential interference contrast and confocal images were obtained with a DM LB2 microscope (Leica, Solms, Germany) and an LSM 510 laser scanning microscope equipped with a Meta detector (Zeiss, Jena, Germany), respectively. Excitation/detection wavelengths used to detect fluorescence were 488/500-550 nm for GFP, 514/535-590 nm for YFP, 543/565-615 nm for mCherry and 458/>560 nm for autofluorescence.

Potassium and cesium measurements

To measure plant K and Cs concentrations, pooled shoot tissues from 3-wk old seedlings grown on control medium (~20 mM K^+) or medium supplemented with 2 mM Cs^+ or 40 mM K^+ were processed as previously described (Remy et al. 2012). The K and/or Cs concentration of the digests was quantified by Atomic Emission Spectrometry - Flame (AAnalyst 300, Perkin-Elmer, Waltham, MA, USA) at the Laboratório de Análises, Instituto Superior Técnico (Lisbon, Portugal) according to methods SMEWW 3500-K B and SMEWW 3500-Cs, respectively, described by Eaton et al. (2005). K

and Cs standards for analytical calibration were from Merck KGaA (Darmstadt, Germany). Four independent samples were processed per genotype.

Funding

This work was supported by Fundação para a Ciência e a Tecnologia [EXPL/AGR-PRO/1013/2013 and SFRH/BPD/44640/2008 to E.R, SFRH/BPD/81221/2011 to T.R.C.].

Disclosures

Conflicts of interest: No conflicts of interest declared.

Acknowledgements

We thank Mathias Zeidler and Dániel Shilavy for the pBIN-NA plasmid, Christopher Cobbett and Scott Sinclair for *zif1-2 zifl2-1* mutant seeds, Miguel Baião for technical assistance, as well as Raquel Carvalho and Vera Nunes for help and support.

References

Abel, S. and Theologis, A. (1994) Transient transformation of Arabidopsis leaf protoplasts: a versatile experimental system to study gene expression. *Plant J* 5: 421-427.

Adams, E., Abdollahi, P. and Shin, R. (2013) Cesium Inhibits Plant Growth through Jasmonate Signaling in *Arabidopsis thaliana*. *Int J Mol Sci* 14: 4545-4559.

Ahmad, I. and Maathuis, F.J. (2014) Cellular and tissue distribution of potassium: Physiological relevance, mechanisms and regulation. *J Plant Physiol* 171: 708-714.

Ahn, S.J., Shin, R. and Schachtman, D.P. (2004) Expression of KT/KUP genes in Arabidopsis and the role of root hairs in K+ uptake. *Plant Physiol* 134: 1135-1145.

Aleman, F., Nieves-Cordones, M., Martinez, V. and Rubio, F. (2011) Root K(+) acquisition in plants: the *Arabidopsis thaliana* model. *Plant Cell Physiol* 52: 1603-1612.

Ali, R., Zielinski, R.E. and Berkowitz, G.A. (2006) Expression of plant cyclic nucleotide-gated cation channels in yeast. *J Exp Bot* 57: 125-138.

Amtmann, A., Troufflard, S. and Armengaud, P. (2008) The effect of potassium nutrition on pest and disease resistance in plants. *Physiol Plant* 133: 682-691.

Anderson, J.A., Huprikar, S.S., Kochian, L.V., Lucas, W.J. and Gaber, R.F. (1992) Functional expression of a probable *Arabidopsis thaliana* potassium channel in *Saccharomyces cerevisiae*. *Proc Natl Acad Sci U S A* 89: 3736-3740.

Anschutz, U., Becker, D. and Shabala, S. (2014) Going beyond nutrition: Regulation of potassium homoeostasis as a common denominator of plant adaptive responses to environment. *J Plant Physiol* 171: 670-687.

Ashley, M.K., Grant, M. and Grabov, A. (2006) Plant responses to potassium deficiencies: a role for potassium transport proteins. *J Exp Bot* 57: 425-436.

Barragan, V., Leidi, E.O., Andres, Z., Rubio, L., De Luca, A., Fernandez, J.A., et al. (2012) Ion exchangers NHX1 and NHX2 mediate active potassium uptake into vacuoles to regulate cell turgor and stomatal function in Arabidopsis. *Plant Cell* 24: 1127-1142.

Bassil, E., Tajima, H., Liang, Y.C., Ohto, M.A., Ushijima, K., Nakano, R., et al. (2011) The Arabidopsis Na+/H+ antiporters NHX1 and NHX2 control vacuolar pH and K+ homeostasis to regulate growth, flower development, and reproduction. *Plant Cell* 23: 3482-3497.

Becker, D., Dreyer, I., Hoth, S., Reid, J.D., Busch, H., Lehnen, M., et al. (1996) Changes in voltage activation, Cs+ sensitivity, and ion permeability in H5 mutants of the plant K+ channel KAT1. *Proc Natl Acad Sci U S A* 93: 8123-8128.

Becker, D., Geiger, D., Dunkel, M., Roller, A., Bertl, A., Latz, A., et al. (2004) AtTPK4, an Arabidopsis tandem-pore K+ channel, poised to control the pollen membrane voltage in a pH- and Ca2+-dependent manner. *Proc Natl Acad Sci U S A* 101: 15621-15626.

Borsics, T., Webb, D., Andeme-Ondzighi, C., Staehelin, L.A. and Christopher, D.A. (2007) The cyclic nucleotide-gated calmodulin-binding channel AtCNGC10 localizes to the plasma membrane and influences numerous growth responses and starch accumulation in *Arabidopsis thaliana*. *Planta* 225: 563-573.

Broadley, M.R., Escobar-Gutierrez, A.J., Bowen, H.C., Willey, N.J. and White, P.J. (2001) Influx and accumulation of Cs(+) by the akt1 mutant of *Arabidopsis thaliana* (L.) Heynh. lacking a dominant K(+) transport system. *J Exp Bot* 52: 839-844.

Buttner, M. (2007) The monosaccharide transporter(-like) gene family in Arabidopsis. *FEBS Lett* 581: 2318-2324.

Cabrito, T.R., Teixeira, M.C., Duarte, A.A., Duque, P. and Sá-Correia, I. (2009) Heterologous expression of a Tpo1 homolog from *Arabidopsis thaliana* confers resistance to the herbicide 2,4-D and other chemical stresses in yeast. *Appl Microbiol Biotechnol* 84: 927-936.

Cellier, F., Conejero, G., Ricaud, L., Luu, D.T., Lepetit, M., Gosti, F., et al. (2004) Characterization of AtCHX17, a member of the cation/H+ exchangers, CHX family, from *Arabidopsis thaliana* suggests a role in K+ homeostasis. *Plant J* 39: 834-846.

Chanroj, S., Lu, Y., Padmanaban, S., Nanatani, K., Uozumi, N., Rao, R., et al. (2011) Plant-specific cation/H+ exchanger 17 and its homologs are endomembrane K+ transporters with roles in protein sorting. *J Biol Chem* 286: 33931-33941.

Clough, S.J. and Bent, A.F. (1998) Floral dip: a simplified method for Agrobacterium-mediated transformation of *Arabidopsis thaliana*. *Plant J* 16: 735-743.

Deeken, R., Geiger, D., Fromm, J., Koroleva, O., Ache, P., Langenfeld-Heyser, R., et al. (2002) Loss of the AKT2/3 potassium channel affects sugar loading into the phloem of Arabidopsis. *Planta* 216: 334-344.

Desbrosses, G., Josefsson, C., Rigas, S., Hatzopoulos, P. and Dolan, L. (2003) AKT1 and TRH1 are required during root hair elongation in Arabidopsis. *J Exp Bot* 54: 781-788.

do Valle Matta, M.A., Jonniaux, J.L., Balzi, E., Goffeau, A. and van den Hazel, B. (2001) Novel target genes of the yeast regulator Pdr1p: a contribution of the TPO1 gene in resistance to quinidine and other drugs. *Gene* 272: 111-119.

Eaton, A.D., Clesceri, L.S., Rice, E.W. and Greenberg, A.E., eds. (2005) *Standard Methods for the Examination of Water and Wastewater*. American Public Health Association, American Water Works Association, Water Environment Federation.

Elumalai, R.P., Nagpal, P. and Reed, J.W. (2002) A mutation in the Arabidopsis KT2/KUP2 potassium transporter gene affects shoot cell expansion. *Plant Cell* 14: 119-131.

Evans, A.R., Hall, D., Pritchard, J. and Newbury, H.J. (2012) The roles of the cation transporters CHX21 and CHX23 in the development of *Arabidopsis thaliana*. *J Exp Bot* 63: 59-67.

Fankhauser, C. and Casal, J.J. (2004) Phenotypic characterization of a photomorphogenic mutant. *Plant J* 39: 747-760.

Fu, H.H. and Luan, S. (1998) AtKuP1: a dual-affinity K+ transporter from Arabidopsis. *Plant Cell* 10: 63-73.

Gajdanowicz, P., Michard, E., Sandmann, M., Rocha, M., Correa, L.G., Ramirez-Aguilar, S.J., et al. (2011) Potassium (K+) gradients serve as a mobile energy source in plant vascular tissues. *Proc Natl Acad Sci U S A* 108: 864-869.

Gaymard, F., Pilot, G., Lacombe, B., Bouchez, D., Bruneau, D., Boucherez, J., et al. (1998) Identification and disruption of a plant shaker-like outward channel involved in K+ release into the xylem sap. *Cell* 94: 647-655.

Gierth, M., Maser, P. and Schroeder, J.I. (2005) The potassium transporter AtHAK5 functions in K(+) deprivation-induced high-affinity K(+) uptake and AKT1 K(+) channel contribution to K(+) uptake kinetics in Arabidopsis roots. *Plant Physiol* 137: 1105-1114.

Gobert, A., Isayenkov, S., Voelker, C., Czempinski, K. and Maathuis, F.J. (2007) The two-pore channel TPK1 gene encodes the vacuolar K+ conductance and plays a role in K+ homeostasis. *Proc Natl Acad Sci U S A* 104: 10726-10731.

Gobert, A., Park, G., Amtmann, A., Sanders, D. and Maathuis, F.J. (2006) *Arabidopsis thaliana* cyclic nucleotide gated channel 3 forms a non-selective ion transporter involved in germination and cation transport. *J Exp Bot* 57: 791-800.

Guo, K.M., Babourina, O., Christopher, D.A., Borsics, T. and Rengel, Z. (2008) The cyclic nucleotide-gated channel, AtCNGC10, influences salt tolerance in Arabidopsis. *Physiol Plant* 134: 499-507.

Hampton, C.R., Bowen, H.C., Broadley, M.R., Hammond, J.P., Mead, A., Payne, K.A., et al. (2004) Cesium toxicity in Arabidopsis. *Plant Physiol* 136: 3824-3837.

Haydon, M.J. and Cobbett, C.S. (2007) A novel major facilitator superfamily protein at the tonoplast influences zinc tolerance and accumulation in Arabidopsis. *Plant Physiol* 143: 1705-1719.

Haydon, M.J., Kawachi, M., Wirtz, M., Hillmer, S., Hell, R. and Kramer, U. (2012) Vacuolar nicotianamine has critical and distinct roles under iron deficiency and for zinc sequestration in Arabidopsis. *Plant Cell* 24: 724-737.

Hirsch, R.E., Lewis, B.D., Spalding, E.P. and Sussman, M.R. (1998) A role for the AKT1 potassium channel in plant nutrition. *Science* 280: 918-921.

Hosy, E., Vavasseur, A., Mouline, K., Dreyer, I., Gaymard, F., Poree, F., et al. (2003) The Arabidopsis outward K+ channel GORK is involved in regulation of stomatal movements and plant transpiration. *Proc Natl Acad Sci U S A* 100: 5549-5554.

Ivashikina, N., Becker, D., Ache, P., Meyerhoff, O., Felle, H.H. and Hedrich, R. (2001) K(+) channel profile and electrical properties of Arabidopsis root hairs. *FEBS Lett* 508: 463-469.

Jansen, G., Wu, C., Schade, B., Thomas, D.Y. and Whiteway, M. (2005) Drag&Drop cloning in yeast. *Gene* 344: 43-51.

Kanter, U., Hauser, A., Michalke, B., Draxl, S. and Schaffner, A.R. (2010) Caesium and strontium accumulation in shoots of *Arabidopsis thaliana*: genetic and physiological aspects. *J Exp Bot* 61: 3995-4009.

Karimi, M., Inze, D. and Depicker, A. (2002) GATEWAY vectors for Agrobacterium-mediated plant transformation. *Trends Plant Sci* 7: 193-195.

Kim, E.J., Kwak, J.M., Uozumi, N. and Schroeder, J.I. (1998) AtKUP1: an Arabidopsis gene encoding high-affinity potassium transport activity. *Plant Cell* 10: 51-62.

Kneen, M., Farinas, J., Li, Y. and Verkman, A.S. (1998) Green fluorescent protein as a noninvasive intracellular pH indicator. *Biophys J* 74: 1591-1599.

Kobayashi, D., Uozumi, N., Hisamatsu, S. and Yamagami, M. (2010) AtKUP/HAK/KT9, a K+ transporter from *Arabidopsis thaliana*, mediates Cs+ uptake in *Escherichia coli*. *Biosci Biotechnol Biochem* 74: 203-205.

Kohler, C., Merkle, T. and Neuhaus, G. (1999) Characterisation of a novel gene family of putative cyclic nucleotide- and calmodulin-regulated ion channels in *Arabidopsis thaliana*. *Plant J* 18: 97-104.

Krogh, A., Larsson, B., von Heijne, G. and Sonnhammer, E.L. (2001) Predicting transmembrane protein topology with a hidden Markov model: application to complete genomes. *J Mol Biol* 305: 567-580.

Kwak, J.M., Murata, Y., Baizabal-Aguirre, V.M., Merrill, J., Wang, M., Kemper, A., et al. (2001) Dominant negative guard cell K+ channel mutants reduce inward-rectifying K+ currents and light-induced stomatal opening in arabidopsis. *Plant Physiol* 127: 473-485.

Leigh, R.A. and Jones, R.G.W. (1984) A Hypothesis Relating Critical Potassium Concentrations for Growth to the Distribution and Functions of This Ion in the Plant-Cell. *New Phytol* 97: 1-13.

Liu, H., Tang, R., Zhang, Y., Wang, C., Lv, Q., Gao, X., et al. (2010) AtNHX3 is a vacuolar K+/H+ antiporter required for low-potassium tolerance in *Arabidopsis thaliana*. *Plant Cell Environ* 33: 1989-1999.

Liu, J. and Zhu, J.K. (1997) An Arabidopsis mutant that requires increased calcium for potassium nutrition and salt tolerance. *Proc Natl Acad Sci U S A* 94: 14960-14964.

Lu, Y., Chanroj, S., Zulkifli, L., Johnson, M.A., Uozumi, N., Cheung, A., et al. (2011) Pollen tubes lacking a pair of K+ transporters fail to target ovules in Arabidopsis. *Plant Cell* 23: 81-93.

Maathuis, F.J. (2009) Physiological functions of mineral macronutrients. *Curr Opin Plant Biol* 12: 250-258.

Maresova, L. and Sychrova, H. (2006) *Arabidopsis thaliana* CHX17 gene complements the kha1 deletion phenotypes in *Saccharomyces cerevisiae*. *Yeast* 23: 1167-1171.

Marschner, P., ed. (2012) *Mineral Nutrition of Higher Plants*. Academic Press, London.

Mouline, K., Very, A.A., Gaymard, F., Boucherez, J., Pilot, G., Devic, M., et al. (2002) Pollen tube development and competitive ability are impaired by disruption of a Shaker K(+) channel in Arabidopsis. *Genes Dev* 16: 339-350.

Murashige, T. and Skoog, F. (1962) A revised medium for rapid growth and bioassays with tobacco tissue culture. *Physiol Plant* 15: 473-497.

Nelson, B.K., Cai, X. and Nebenfuhr, A. (2007) A multicolored set of in vivo organelle markers for co-localization studies in Arabidopsis and other plants. *Plant J* 51: 1126-1136.

Nieves-Cordones, M., Aleman, F., Martinez, V. and Rubio, F. (2010) The *Arabidopsis thaliana* HAK5 K+ transporter is required for plant growth and K+ acquisition from low K+ solutions under saline conditions. *Mol Plant* 3: 326-333.

Nieves-Cordones, M., Caballero, F., Martinez, V. and Rubio, F. (2012) Disruption of the *Arabidopsis thaliana* inward-rectifier K+ channel AKT1 improves plant responses to water stress. *Plant Cell Physiol* 53: 423-432.

Nussaume, L., Kanno, S., Javot, H., Marin, E., Pochon, N., Ayadi, A., et al. (2011) Phosphate import in plants: focus on the PHT1 transporters. *Front Plant Sci* 2: doi: 10.3389/fpls.2011.00083.

Osakabe, Y., Arinaga, N., Umezawa, T., Katsura, S., Nagamachi, K., Tanaka, H., et al. (2013) Osmotic stress responses and plant growth controlled by potassium transporters in Arabidopsis. *Plant Cell* 25: 609-624.

Padmanaban, S., Chanroj, S., Kwak, J.M., Li, X., Ward, J.M. and Sze, H. (2007) Participation of endomembrane cation/H+ exchanger AtCHX20 in osmoregulation of guard cells. *Plant Physiol* 144: 82-93.

Pao, S.S., Paulsen, I.T. and Saier, M.H., Jr. (1998) Major facilitator superfamily. *Microbiol Mol Biol Rev* 62: 1-34.

Pyo, Y.J., Gierth, M., Schroeder, J.I. and Cho, M.H. (2010) High-affinity K(+) transport in Arabidopsis: AtHAK5 and AKT1 are vital for seedling establishment and postgermination growth under low-potassium conditions. *Plant Physiol* 153: 863-875.

Qi, Z., Hampton, C.R., Shin, R., Barkla, B.J., White, P.J. and Schachtman, D.P. (2008) The high affinity K+ transporter AtHAK5 plays a physiological role in planta at very low K+ concentrations and provides a caesium uptake pathway in Arabidopsis. *J Exp Bot* 59: 595-607.

Quintero, F.J. and Blatt, M.R. (1997) A new family of K+ transporters from Arabidopsis that are conserved across phyla. *FEBS Lett* 415: 206-211.

Remy, E., Baster, P., Friml, J. and Duque, P. (2013a) ZIFL1.1 transporter modulates polar auxin transport by stabilizing membrane abundance of multiple PINs in Arabidopsis root tip. *Plant Signal Behav* 8: doi: 10 4161/psb 25688.

Remy, E., Cabrito, T.R., Baster, P., Batista, R.A., Teixeira, M.C., Friml, J., et al. (2013b) A major facilitator superfamily transporter plays a dual role in polar auxin transport and drought stress tolerance in Arabidopsis. *Plant Cell* 25: 901-926.

Remy, E., Cabrito, T.R., Batista, R.A., Hussein, M.A., Teixeira, M.C., Athanasiadis, A., et al. (2014) Intron Retention in the 5'UTR of the Novel ZIF2 Transporter Enhances Translation to Promote Zinc Tolerance in Arabidopsis. *PLoS Genet* 10: e1004375.

Remy, E., Cabrito, T.R., Batista, R.A., Teixeira, M.C., Sa-Correia, I. and Duque, P. (2012) The Pht1;9 and Pht1;8 transporters mediate inorganic phosphate acquisition by the *Arabidopsis thaliana* root during phosphorus starvation. *New Phytol* 195: 356-371.

Rigas, S., Debrosses, G., Haralampidis, K., Vicente-Agullo, F., Feldmann, K.A., Grabov, A., et al. (2001) TRH1 encodes a potassium transporter required for tip growth in Arabidopsis root hairs. *Plant Cell* 13: 139-151.

Rubio, F., Nieves-Cordones, M., Aleman, F. and Martinez, V. (2008) Relative contribution of AtHAK5 and AtAKT1 to K+ uptake in the high-affinity range of concentrations. *Physiol Plant* 134: 598-608.

Rubio, F., Santa-Maria, G.E. and Rodriguez-Navarro, A. (2000) Cloning of Arabidopsis and barley cDNAs encoding HAK potassium transporters in root and shoot cells. *Physiol Plant* 109: 34-43.

Rus, A., Lee, B.H., Munoz-Mayor, A., Sharkhuu, A., Miura, K., Zhu, J.K., et al. (2004) AtHKT1 facilitates Na+ homeostasis and K+ nutrition in planta. *Plant Physiol* 136: 2500-2511.

Sahr, T., Voigt, G., Paretzke, H.G., Schramel, P. and Ernst, D. (2005) Caesium-affected gene expression in *Arabidopsis thaliana*. *New Phytol* 165: 747-754.

Schachtman, D.P., Schroeder, J.I., Lucas, W.J., Anderson, J.A. and Gaber, R.F. (1992) Expression of an inward-rectifying potassium channel by the Arabidopsis KAT1 cDNA. *Science* 258: 1654-1658.

Sentenac, H., Bonneaud, N., Minet, M., Lacroute, F., Salmon, J.M., Gaymard, F., et al. (1992) Cloning and expression in yeast of a plant potassium ion transport system. *Science* 256: 663-665.

Serrano, R. (1978) Characterization of the plasma membrane ATPase of *Saccharomyces cerevisiae*. *Mol Cell Biochem* 22: 51-63.

Sharma, T., Dreyer, I. and Riedelsberger, J. (2013) The role of K(+) channels in uptake and redistribution of potassium in the model plant *Arabidopsis thaliana*. *Front Plant Sci* 4: 224.

Shin, H., Shin, H.S., Dewbre, G.R. and Harrison, M.J. (2004) Phosphate transport in Arabidopsis: Pht1;1 and Pht1;4 play a major role in phosphate acquisition from both low- and high-phosphate environments. *Plant J* 39: 629-642.

Silhavy, D., Molnar, A., Lucioli, A., Szittya, G., Hornyik, C., Tavazza, M., et al. (2002) A viral protein suppresses RNA silencing and binds silencing-generated, 21- to 25-nucleotide double-stranded RNAs. *EMBO J* 21: 3070-3080.

Sundaresan, V., Springer, P., Volpe, T., Haward, S., Jones, J.D., Dean, C., et al. (1995) Patterns of gene action in plant development revealed by enhancer trap and gene trap transposable elements. *Genes Dev* 9: 1797-1810.

Szczerba, M.W., Britto, D.T. and Kronzucker, H.J. (2009) K+ transport in plants: physiology and molecular biology. *J Plant Physiol* 166: 447-466.

Tsay, Y.F., Chiu, C.C., Tsai, C.B., Ho, C.H. and Hsu, P.K. (2007) Nitrate transporters and peptide transporters. *FEBS Lett* 581: 2290-2300.

Vargas, R.C., Garcia-Salcedo, R., Tenreiro, S., Teixeira, M.C., Fernandes, A.R., Ramos, J., et al. (2007) *Saccharomyces cerevisiae* multidrug resistance transporter Qdr2 is implicated in potassium uptake, providing a physiological advantage to quinidine-stressed cells. *Eukaryot Cell* 6: 134-142.

Vicente-Agullo, F., Rigas, S., Desbrosses, G., Dolan, L., Hatzopoulos, P. and Grabov, A. (2004) Potassium carrier TRH1 is required for auxin transport in Arabidopsis roots. *Plant J* 40: 523-535.

Voinnet, O., Rivas, S., Mestre, P. and Baulcombe, D. (2003) An enhanced transient expression system in plants based on suppression of gene silencing by the p19 protein of tomato bushy stunt virus. *Plant J* 33: 949-956.

Ward, J.M. (1982) Spectral Perturbations of the Aequorea Green-Fluorescent Protein. *Photochem Photobiol* 35: 803-808.

White, P.J. and Broadley, M.R. (2000) Mechanisms of ceasium uptake by plants. *New Phytol* 147: 241-256.

White, P.J. and Karley, A.J. (2010) Potassium. In *Cell Biology of Metals and Nutrients*. Edited by Hell, R. and Mendel, R.-R. pp. 199–224. Springer, Heidelberg.

Yoo, S.D., Cho, Y.H. and Sheen, J. (2007) Arabidopsis mesophyll protoplasts: a versatile cell system for transient gene expression analysis. *Nat Protoc* 2: 1565-1572.

Zhao, J., Cheng, N.H., Motes, C.M., Blancaflor, E.B., Moore, M., Gonzales, N., et al. (2008) AtCHX13 is a plasma membrane K+ transporter. *Plant Physiol* 148: 796-807.

Zhu, Y.G. and Smolders, E. (2000) Plant uptake of radiocaesium: a review of mechanisms, regulatioand application. *J Exp Bot* 51: 1635-1645.

Table 1 Growth parameters under control conditions of the different plant lines used in this study

Genotype	Shoot parameters		Root parameters		
	FW (mg/plant)	**CC** (mg/mg plant)	**PRE** (cm)	**LRD** (LR/cm)	**TLRL** (cm)
Col-0	35.51 ± 6.65	1.13 ± 0.18	3.73 ± 0.52	2.02 ± 0.49	3.44 ± 0.31
zifl2-1	34.58 ± 4.82 (0.384)	1.16 ± 0.14 (0.370)	3.94 ± 0.50 (0.134)	1.85 ± 0.22 (0.218)	3.89 ± 1.46 (0.220)
zif1-2	36.28 ± 6.55 (0.416)	1.22 ± 0.19 (0.199)	3.83 ± 0.28 (0.273)	1.94 ± 0.33 (0.365)	3.60 ± 0.43 (0.219)
zifl1-2	34.76 ± 4.09 (0.402)	1.16 ± 0.20 (0.391)	3.69 ± 0.33 (0.397)	1.27 ± 0.16 ($8.9e^{-4}$)	2.08 ± 1.00 ($2.1e^{-3}$)
zif1-2 zifl2-1	35.06 ± 7.62 (0.454)	1.20 ± 0.29 (0.303)	3.52 ± 0.27 (0.089)	2.11 ± 0.43 (0.347)	3.52 ± 1.27 (0.436)
zifl1-2 zifl2-1	34.45 ± 6.98 (0.387)	1.19 ± 0.15 (0.272)	3.83 ± 0.28 (0.279)	1.13 ± 0.09 ($1.7e^{-4}$)	2.32 ± 0.79 ($1.7e^{-3}$)
zifl2-1/*ZIFL2.1*OX1	32.88 ± 8.16 (0.259)	1.04 ± 0.18 (0.168)	3.80 ± 0.36 (0.341)	1.94 ± 0.52 (0.397)	3.60 ± 1.03 (0.352)
zifl2-1/*ZIFL2.1*OX2	34.26 ± 7.82 (0.376)	1.28 ± 0.17 (0.072)	3.42 ± 0.62 (0.071)	2.12 ± 0.36 (0.334)	3.33 ± 0.97 (0.393)
*ZIFL2.1*OX1	35.03 ± 6.06 (0.444)	1.22 ± 0.18 (0.187)	3.69 ± 0.31 (0.397)	1.89 ± 0.56 (0.338)	3.56 ± 1.38 (0.410)
*ZIFL2.1*OX2	37.16 ± 5.40 (0.309)	1.13 ± 0.20 (0.493)	3.52 ± 0.33 (0.093)	2.02 ± 0.37 (0.500)	3.35 ± 0.51 (0.354)

Shoot biomass (fresh weight, FW), chlorophyll content (CC), primary root elongation (PRE), lateral root density (LRD) and total lateral root length (TLRL) of 8-d (PRE), 14-d (LRD, TLRL) or 21-d (FW, CC) old seedlings from the wild type (Col-0), the *zifl2-1, zif1-2, zifl1-2, zif1-2 zifl2-1* and *zifl1-2 zifl2-1* mutants, and two independent complementation (*zifl2-1*/*ZIFL2.1*OX1 and *zifl2-1*/*ZIFL2.1*OX2) and *ZIFL2.1*-overexpressing (*ZIFL2.1*OX1 and *ZIFL2.1*OX2) lines grown on control (~20 mM K^+) medium (means ± SD, n=8 for FW, CC, LRD and TLRL and n=16 for PRE). Numbers between parentheses indicate the P value (comparison with the wild type) obtained by Student's t-test.

Table 2 Functional redundancy between the *Arabidopsis ZIF1*, *ZIFL1* and *ZIFL2* genes

Genotype	250 μM Zn^{2+}	0.03 μM 2,4-D	0.075 μM IAA	3 mM Cs^{+}	60 mM K^{+}
Col-0	79.40 ± 8.52 (a)	54.94 ± 8.40 (a)	65.31 ± 9.60 (a)	55.70 ± 11.9 (a)	63.67 ± 11.8 (a)
zif1-2	54.00 ± 8.68 (b)	55.34 ± 8.35 (a)	65.05 ± 9.02 (a)	57.52 ± 10.3 (a)	62.89 ± 5.49 (a)
zifl1-2	78.75 ± 7.52 (a)	40.67 ± 6.00 (b)	43.76 ± 7.03 (b)	62.13 ± 9.19 (b)	65.69 ± 6.53 (a)
zifl2-1	78.61 ± 11.4 (a)	54.10 ± 8.97 (a)	66.41 ± 7.83 (a)	70.96 ± 7.34 (c)	78.26 ± 7.11 (b)
zif1-2 zifl2-1	52.13 ± 3.93 (b)	56.49 ± 7.10 (a)	66.88 ± 9.91 (a)	69.66 ± 8.74 (c)	79.27 ± 9.43 (b)
zifl1-2 zifl2-1	75.21 ± 10.1 (a)	39.60 ± 7.20 (b)	42.16 ± 11.3 (b)	67.52 ± 8.78 (c)	77.15 ± 7.13 (b)

Primary root elongation of 8-d old seedlings from the wild type (Col-0) and the *zif1-2*, *zifl1-2*, *zifl2-1*, *zif1-2 zifl2-1* and *zifl1-2 zifl2-1* mutants upon Zn, 2,4-D, IAA, Cs and K challenges (means ± SD, n = 16). Results are representative of three independent experiments. Letters between parentheses indicate statistically significant differences between genotypes (P<0.001; Student's t-test).

Figure Legends

Fig. 1 Structure and expression pattern of the *Arabidopsis ZIFL2* gene. (A) exon/intron organization of the *ZIFL2* gene and T-DNA insertion site in the *zifl2-1* mutant. Boxes and lines between boxes denote exons and introns, respectively. The large open triangle depicts the site of the T-DNA insertion. F1, F2, F3, R1, R2 and R3 indicate the location of the primers used to detect *ZIFL2* expression. Scale bar, 200 bp. (B) Structure of the predicted alternative *ZIFL2* transcripts (current genome annotation, TAIR10). Boxes indicate exons with UTRs in grey, and lines between boxes represent introns. Transcript lengths are indicated. Scale bar, 200 nt. (C) RT-PCR profile of *ZIFL2* expression in different *Arabidopsis* wild-type (Col-0) tissues. The location of the F2, R2, F3, R3, F4, R4 and R4' primers used is shown in (A). Expression of the *ROC1* gene was used as a loading control. Results are representative of three independent experiments. (D) Differential interference contrast microscopy images of GUS-stained primary roots of a wild type (left panel) or a transgenic plant carrying the Pro*ZIFL2:GFP: GUS* reporter construct (right panel). Scale bar, 50 *μ*m.

Fig. 2 Subcellular localization of the *Arabidopsis* ZIFL2.1 transporter. (A-B) Confocal laser scanning microscopy images of wild-type *Arabidopsis* mesophyll protoplasts transiently expressing either YFP alone (A) or the ZIFL2.1-YFP fusion (B) under the control of the 35S promoter. The YFP and chloroplast autofluorescence signals are visualized by green and red coloration, respectively. Scale bars, 10 *μ*m. (C-Q) Confocal laser scanning microscopy images of tobacco leaf epidermal cells transiently co-expressing the ZIFL2.1-GFP fusion (C, F, I, L, O) with the tonoplast marker γ-TIP-mCherry (D, G, J) or the plasma membrane marker PIP2A-mCherry (M, P) under the control of the 35S promoter. Merged images of whole-cell views (E, N) or close-ups (H, K, Q) are shown. Arrowheads point to transvacuolar strands and asterisks indicate fluorescence signals approaching the nucleus only on the side facing the exterior of the cell. The GFP and mCherry signals are visualized by green and red coloration, respectively. Scale bars, 20 μm (C, F, L) and 10 *μ*m (I, O).

Fig. 3 Heterologous expression of the *Arabidopsis* ZIFL2.1 transporter in *S. cerevisiae*. (A) Fluorescence microscopy images of exponential-phase yeast *Δtpo1* mutant cells harboring either the cloning vector *pGREG576* (background fluorescence) or the *pGREG576_ZIFL2.1* plasmid after induction of recombinant protein production (upper panels) and corresponding immunoblot analysis of

the GFP-ZIFL2.1 fusion protein using anti-GFP antibodies (lower panel). A representative image of wild-type cells expressing a GFP fusion of the yeast plasma membrane localized Qdr2 transporter is shown as a control. Scale bars, 2 μm. (B) Susceptibility to acetate, malate, Tl^{3+}, Al^{3+} and Cs^{+} of yeast *Δtpo1* mutant cells harboring either the cloning vector *pGREG576* or the *pGREG576_ZIFL2.1* plasmid, as determined by spotting dilution series of cell suspensions (1, 1:5 and 1:10). Results are representative of three independent experiments. (C) Susceptibility to low K^{+} growth conditions of yeast *Δqdr2* mutant cells harboring either the cloning vector *pGREG576* or the *pGREG576_ZIFL2.1* or *pGREG576_ZIFL1.1* plasmids, as determined by spotting dilution series of cell suspensions (1, 1:5 and 1:10). Results are representative of three independent experiments. (D) External medium acidification promoted by energized yeast *Δqdr2* mutant cells harboring either the cloning vector *pGREG576* or the *pGREG576_ZIFL2.1* or *pGREG576_ZIFL1.1* plasmids. Results are representative of three independent experiments.

Fig. 4 Cesium- and potassium-related phenotypes of an *Arabidopsis ZIFL2* loss-of-function mutant. (A) RT-PCR analysis of *ZIFL2* expression in 14-d old wild-type (Col-0) and *zifl2-1* mutant seedlings. The location of the F1, R1, F2, R2, F4, R4 and R4' primers used is shown in Fig 1A. Expression of the *UBQ10* gene was used as a loading control. (B) Representative images of 10-d old wild-type (Col-0) and *zifl2-1* mutant seedlings grown on control medium (~20 mM K^{+}) or under Cs^{+} or excess K^{+} supply. (C) Effect of Cs^{+} (left panels) and K^{+} (right panels) toxicity on shoot biomass (upper panels), chlorophyll content (middle panels) and primary root (PR) elongation (lower panels) of wild-type (Col-0) and *zifl2-1* mutant seedlings (means ± SD, n = 8 for shoot biomass/chlorophyll content and n = 16 for PR elongation). Results are representative of three independent experiments. Asterisks denote statistically significant differences between the two genotypes (* P<0.05, ** P<0.01, *** P<0.001; Student's t-test).

Fig. 5 Cesium- and potassium-related phenotypes of transgenic *Arabidopsis* lines overexpressing *ZIFL2.1*. (A) RT-PCR analysis of *ZIFL2* expression in 14-d old seedlings of the wild type (Col-0) and of two independent complementation (*zifl2-1*/*ZIFL2.1*OX1 and *zifl2-1*/*ZIFL2.1*OX2) and *ZIFL2.1*-overexpressing (*ZIFL2.1*OX1 and *ZIFL2.1*OX2) lines. The location of the F2 and R2 primers used is shown in Figure 1*A*. Expression of the *UBQ10* gene was used as a loading control. Results are representative of three independent experiments. (B) Representative images of 10-d old seedlings of

the wild type (Col-0) and of two independent complementation (*zifl2-1*/*ZIFL2.1*OX1 and *zifl2-1*/*ZIFL2.1*OX2) and *ZIFL2.1*-overexpressing (*ZIFL2.1*OX1 and *ZIFL2.1*OX2) lines grown on control medium (~20 mM K^+) or under Cs^+ or excess K^+ supply. (C) Effect of Cs^+ (middle panels) and K^+ (right panels) toxicity on shoot biomass (upper panels), chlorophyll content (middle panels) and primary root (PR) elongation (lower panels) of seedlings of the wild type (Col-0) and of two independent complementation (*zifl2-1*/*ZIFL2.1*OX1 and *zifl2-1*/*ZIFL2.1*OX2) and *ZIFL2.1*-overexpressing (*ZIFL2.1*OX1 and *ZIFL2.1*OX2) lines (means ± SD, n = 8 for shoot biomass/chlorophyll content and n = 16 for PR elongation). Results are representative of three independent experiments. Asterisks denote statistically significant differences from the wild type under each condition (* P<0.05, ** P<0.01, *** P<0.001; Student's t-test).

Fig. 6 Cesium and potassium content of *Arabidopsis* wild-type, *zifl2-1* mutant and *ZIFL2.1*-ovexpressing lines. (A) Total Cs accumulation, expressed on a dry weight (DW) basis, in the shoot of seedlings of the wild type (Col-0) and the *zifl2-1* mutant as well as of two independent complementation (*zifl2-1*/*ZIFL2.1*OX1 and *zifl2-1*/*ZIFL2.1*OX2) and one *ZIFL2.1*-overexpressing (*ZIFL2.1*OX1) lines grown under 2 mM Cs^+ supply. Bars represent means ± SD, n = 4. Different letters indicate statistically significant differences between genotypes (P<0.05; Student's t-test). (B) K concentration, expressed on a dry weight (DW) basis, in the shoot of 21-d old seedlings of the wild type (Col-0) and the *zifl2-1* mutant as well as of two independent complementation (*zifl2-1*/*ZIFL2.1*OX1 and *zifl2-1*/*ZIFL2.1*OX2) and one *ZIFL2.1*-overexpressing (*ZIFL2.1*OX1) lines grown on control medium (~20 mM K^+) or under Cs^+ or excess K^+ supply. Bars represent means ± SD, n = 4. Different letters indicate statistically significant differences between genotypes under each condition (P<0.05; Student's t-test).

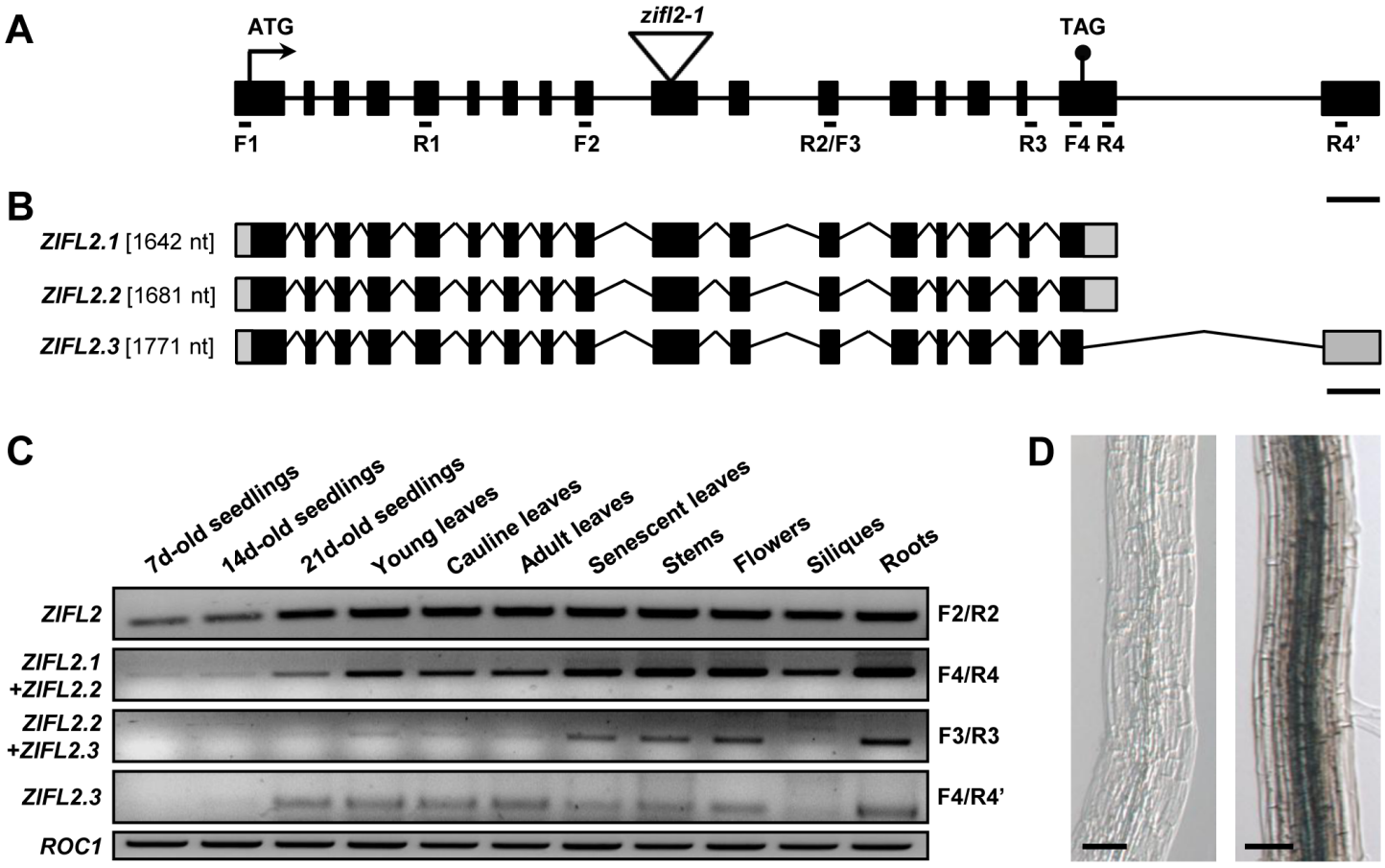
A
ATG
zifl2-1
TAG
F1
R1
F2
R2/F3
R3
F4 R4
R4'
B
ZIFL2.1 [1642 nt]
ZIFL2.2 [1681 nt]
ZIFL2.3 [1771 nt]
C
7d-old seedlings
14d-old seedlings
21d-old seedlings
Young leaves
Cauline leaves
Adult leaves
Senescent leaves
Stems
Flowers
Siliques
Roots
ZIFL2
ZIFL2.1 +ZIFL2.2
ZIFL2.2 +ZIFL2.3
ZIFL2.3
ROC1
F2/R2
F4/R4
F3/R3
F4/R4'
D

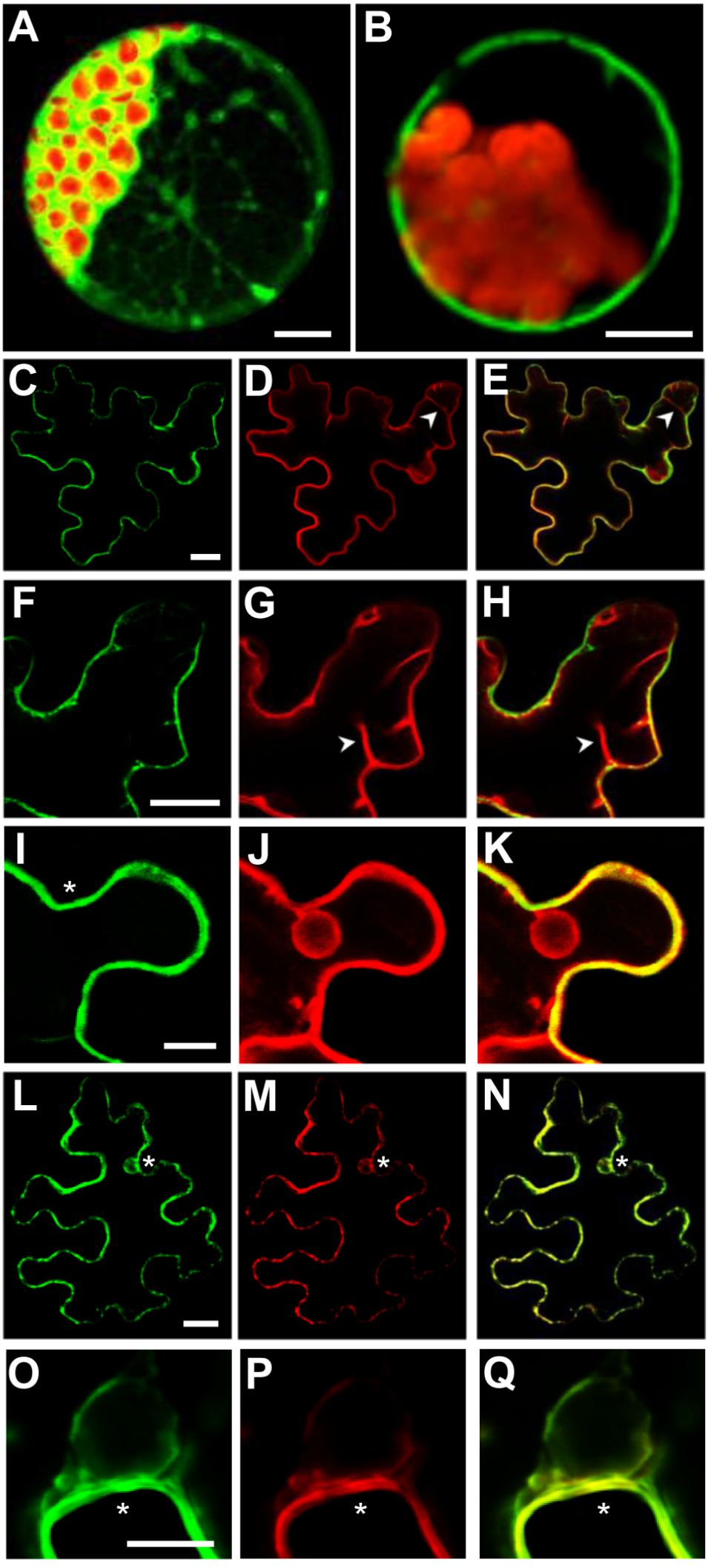
A
B
C
D
E
F
G
H
I
J
K
L
M
N
O
P
Q

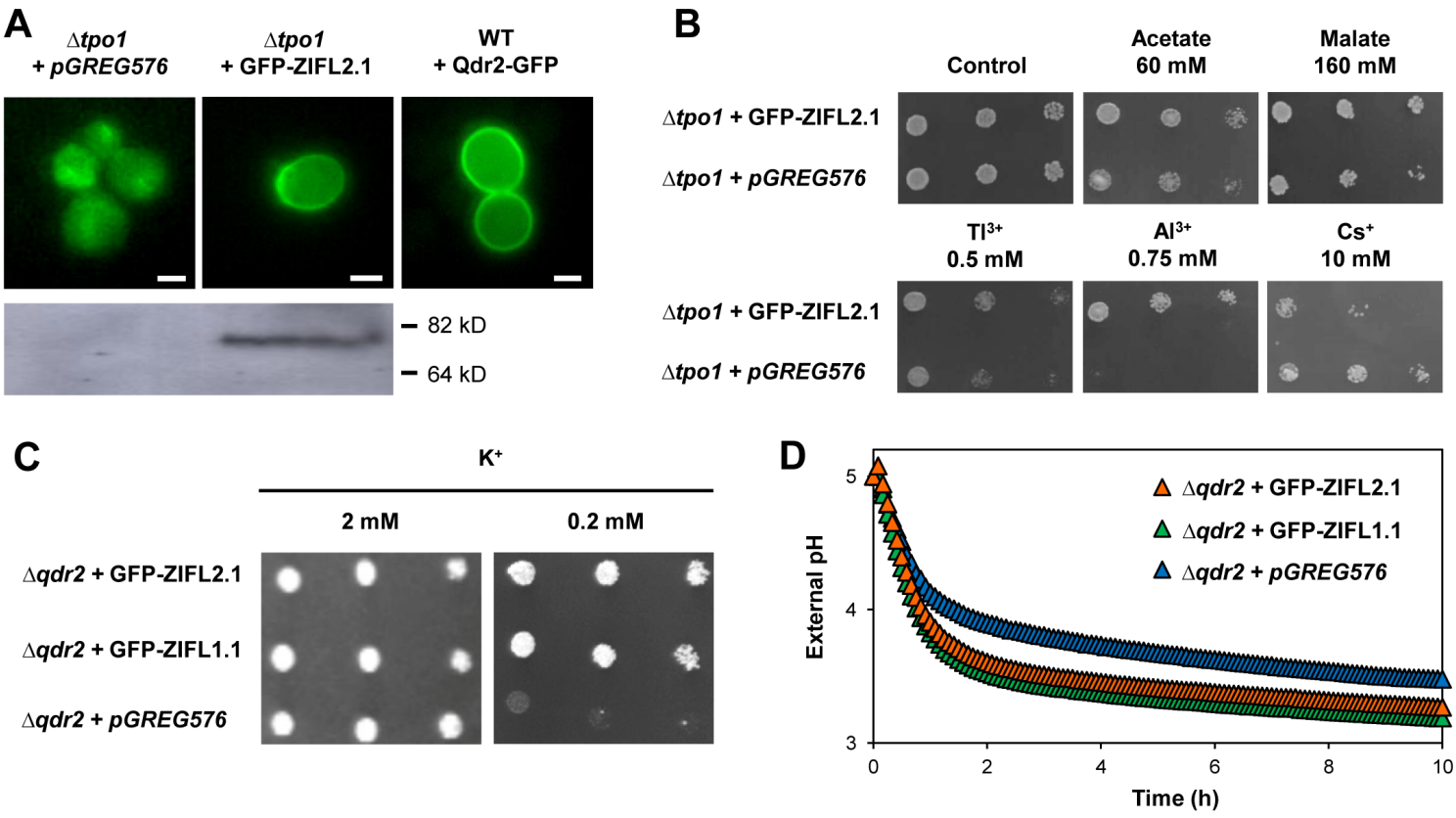
A
Δtpo1 + pGREG576
Δtpo1 + GFP-ZIFL2.1
WT + Qdr2-GFP
82 kD
64 kD
B
Control
Acetate 60 mM
Malate 160 mM
Δtpo1 + GFP-ZIFL2.1
Δtpo1 + pGREG576
Tl3+ 0.5 mM
Al3+ 0.75 mM
Cs+ 10 mM
Δtpo1 + GFP-ZIFL2.1
Δtpo1 + pGREG576
C
K+
2 mM
0.2 mM
Δqdr2 + GFP-ZIFL2.1
Δqdr2 + GFP-ZIFL1.1
Δqdr2 + pGREG576
D
Δqdr2 + GFP-ZIFL2.1
Δqdr2 + GFP-ZIFL1.1
Δqdr2 + pGREG576
External pH
Time (h)
5
4
3
0
2
4
6
8
10

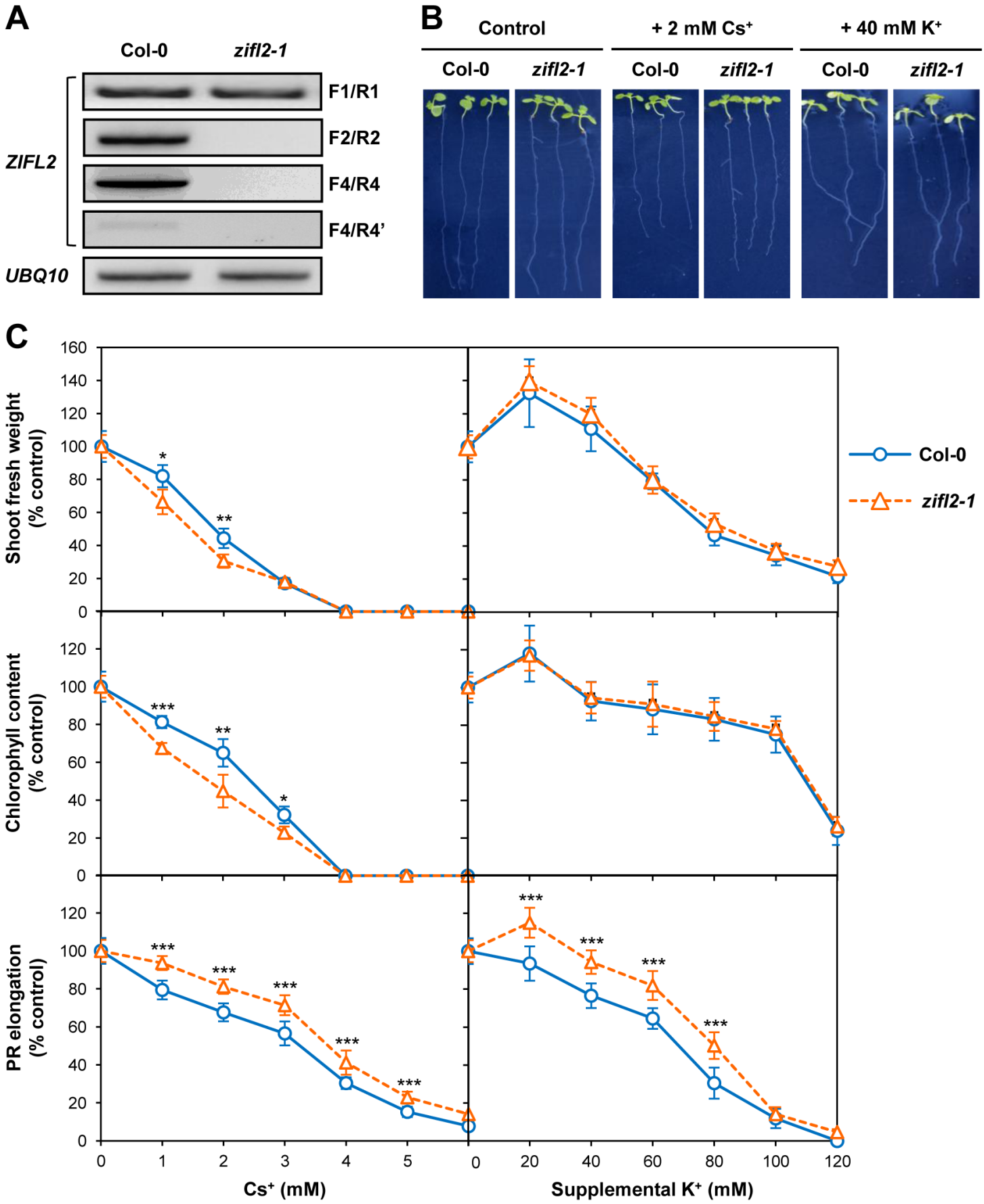
A
Col-0
zifl2-1
ZIFL2
F1/R1
F2/R2
F4/R4
F4/R4'
UBQ10
B
Control
+ 2 mM Cs+
+ 40 mM K+
Col-0
zifl2-1
Col-0
zifl2-1
Col-0
zifl2-1
C
Shoot fresh weight (% control)
Chlorophyll content (% control)
PR elongation (% control)
Col-0
zifl2-1
Cs+ (mM)
Supplemental K+ (mM)

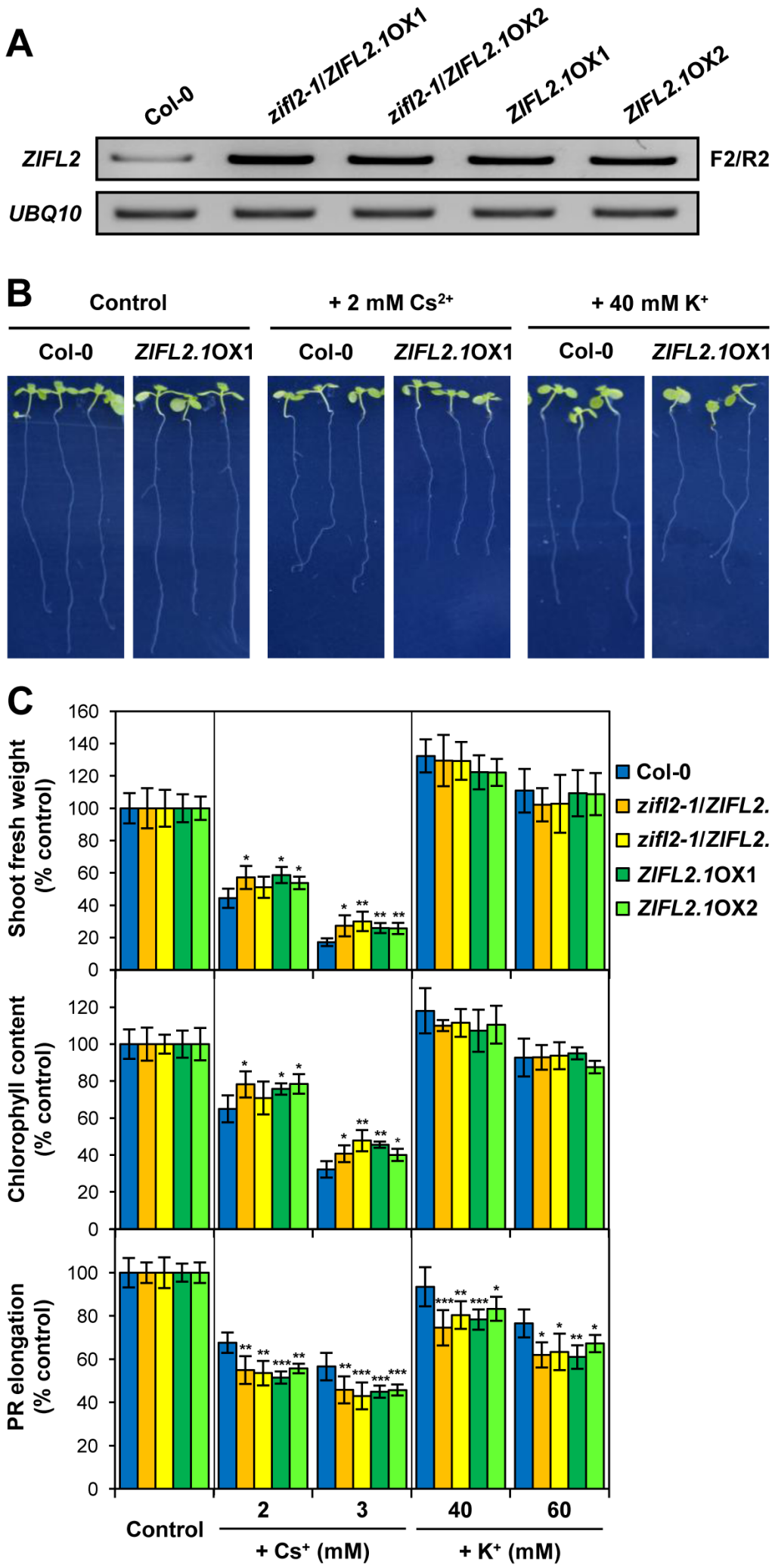
A
Col-0
zifl2-1/ZIFL2.1OX1
zifl2-1/ZIFL2.1OX2
ZIFL2.1OX1
ZIFL2.1OX2
ZIFL2
UBQ10
F2/R2
B
Control
+ 2 mM Cs2+
+ 40 mM K+
Col-0
ZIFL2.1OX1
Col-0
ZIFL2.1OX1
Col-0
ZIFL2.1OX1
C
Shoot fresh weight (% control)
Chlorophyll content (% control)
PR elongation (% control)
Col-0
zifl2-1/ZIFL2.1OX1
zifl2-1/ZIFL2.1OX2
ZIFL2.1OX1
ZIFL2.1OX2
Control
2
3
40
60
+ Cs+ (mM)
+ K+ (mM)

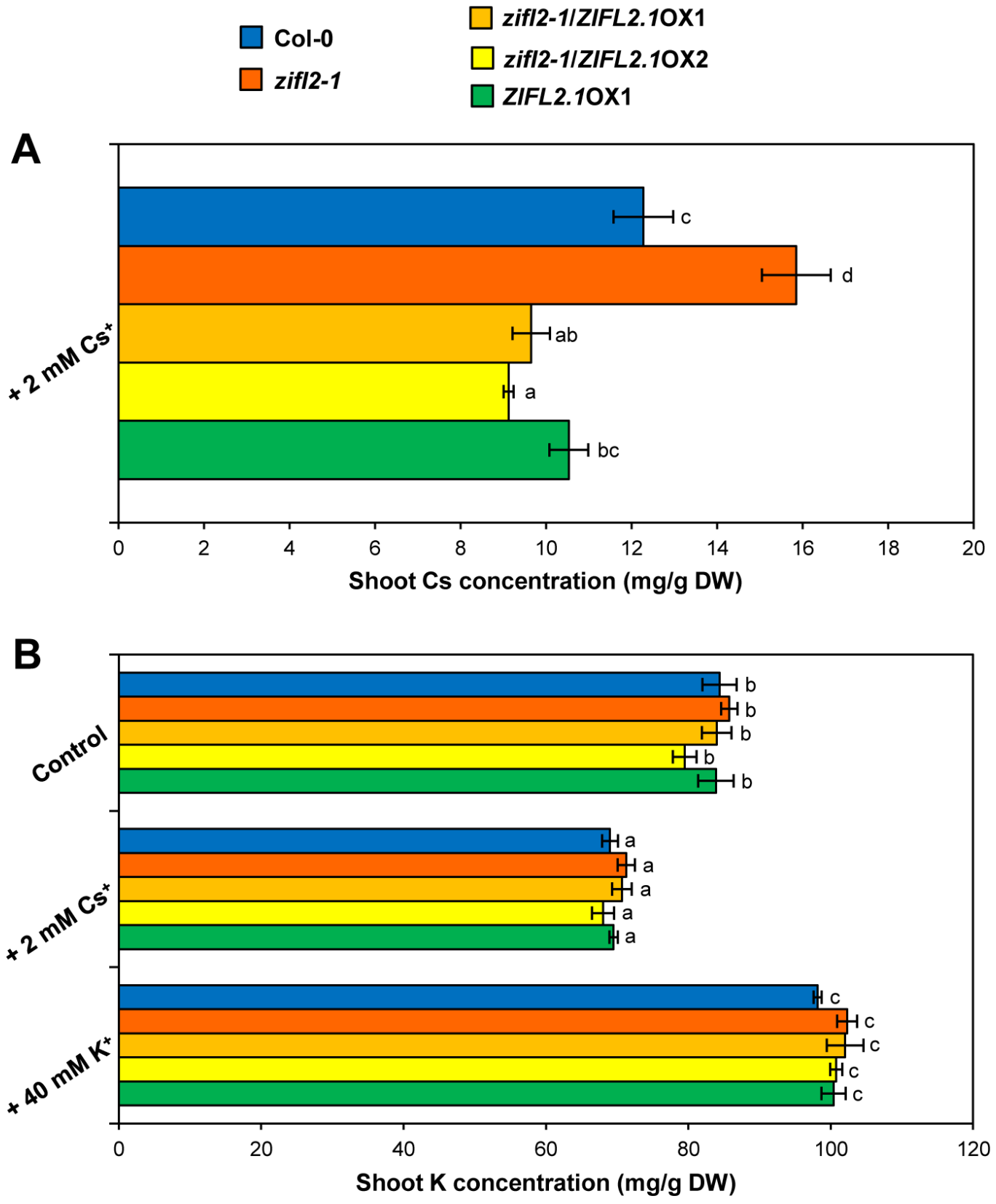
Col-0
zifl2-1
zifl2-1/ZIFL2.1OX1
zifl2-1/ZIFL2.1OX2
ZIFL2.1OX1
A
+ 2 mM Cs+
c
d
ab
a
bc
0
2
4
6
8
10
12
14
16
18
20
Shoot Cs concentration (mg/g DW)
B
Control
+ 2 mM Cs+
+ 40 mM K+
b
b
b
b
b
a
a
a
a
a
c
c
c
c
c
0
20
40
60
80
100
120
Shoot K concentration (mg/g DW)

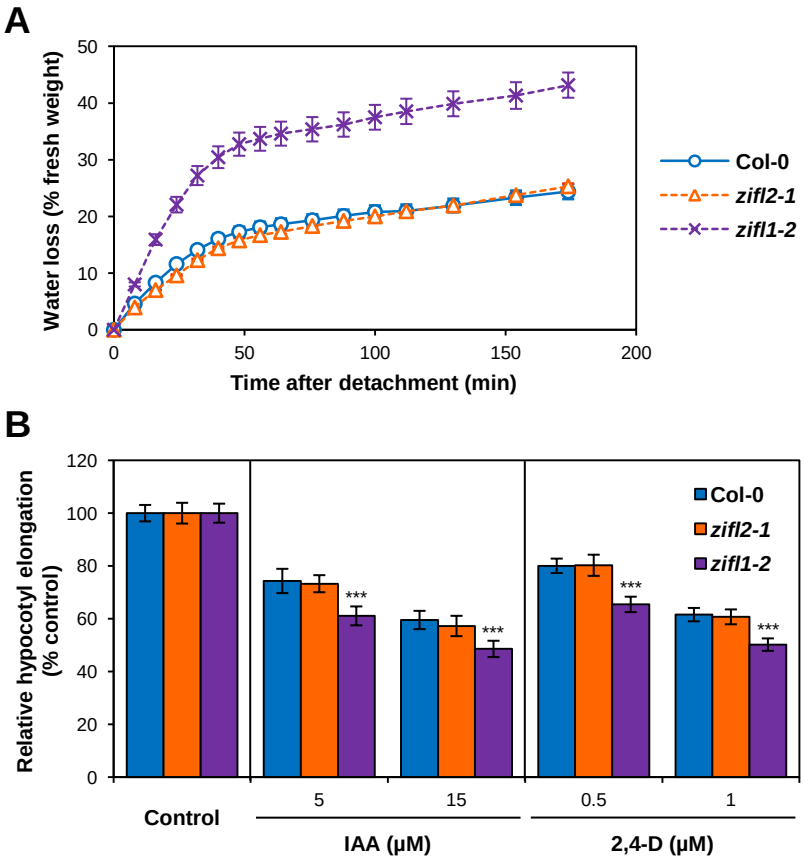

Fig. S1 Drought- and auxin-related phenotypes of an *Arabidopsis ZIFL2* loss-of-function mutant. (A) Water loss rates of rosette leaves detached from 5-week-old irrigated plants of the wild type (Col-0) and the *zifl2-1* and *zifl1-2* mutants (means ± SD, n = 3). Results are representative of two independent experiments. (B) Effect of IAA and 2,4-D on hypocotyl elongation of 7-d-old dark-grown seedlings of the wild type (Col-0) and the *zifl2-1* and *zifl1-2* mutants (means ± SD, *n* = 40-60). Results are representative of two independent repetitions. Asterisks denote statistically significant differences between the two genotypes (*** *P*<0.001; Student's *t*-test).

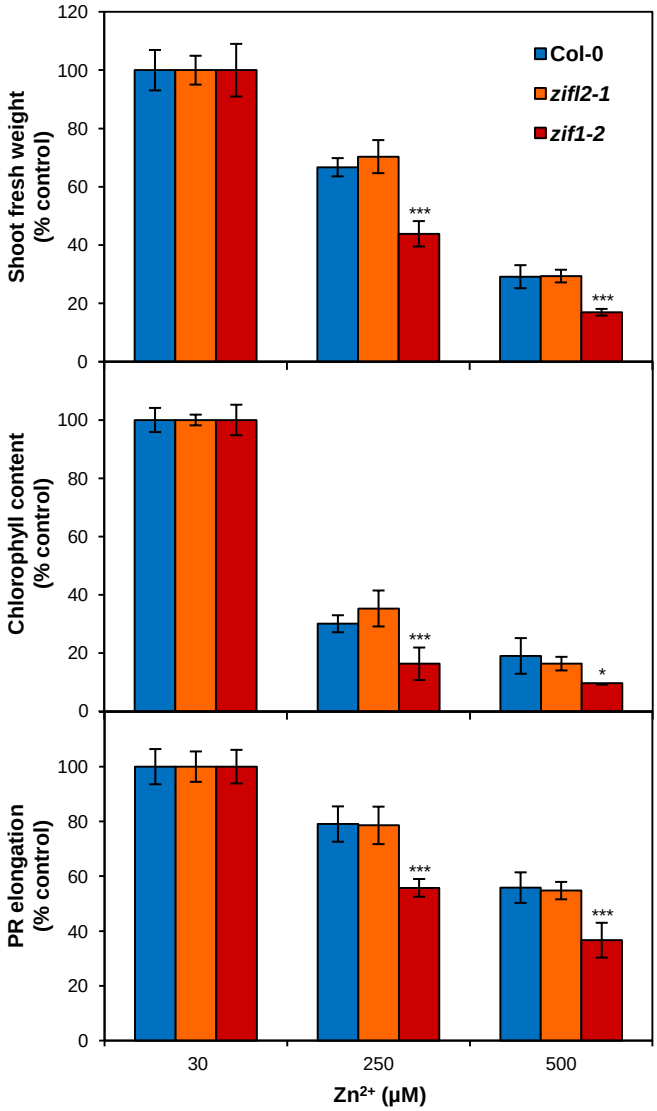

Fig. S2 Zinc-related phenotype of an *Arabidopsis ZIFL2* loss-of-function mutant. Effect of Zn toxicity on shoot biomass (upper panel), chlorophyll content (middle panel) and primary root (PR) elongation (lower panel) of seedlings from the wild type (Col-0) and the *zifl2-1* and *zif1-2* mutants. Results are representative of two independent experiments (means ± SD, n = 8 for shoot biomass/chlorophyll content and n = 16 for PR elongation). Asterisks denote statistically significant differences from the wild type (* P<0.05; *** P<0.001; Student's t-test).

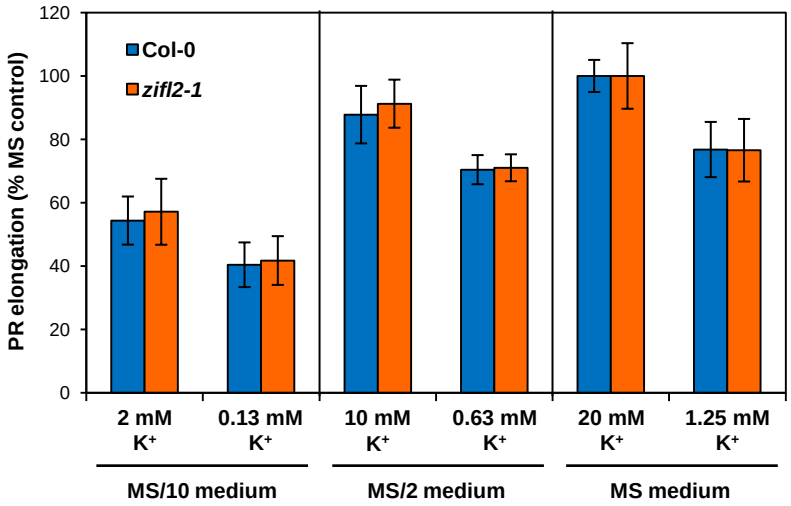

Fig. S3 Potassium deficiency-related phenotype of an *Arabidopsis ZIFL2* loss-of-function mutant. Effect of K^+ deficiency under different MS strengths on PR elongation of wild-type (Col-0) and *zifl2-1* mutant seedlings. Results are representative of two independent experiments and values represent means ± SD (n=8). No statistical differences between mutant and wild type were detected under each condition (P>0.05; Student's t-test).

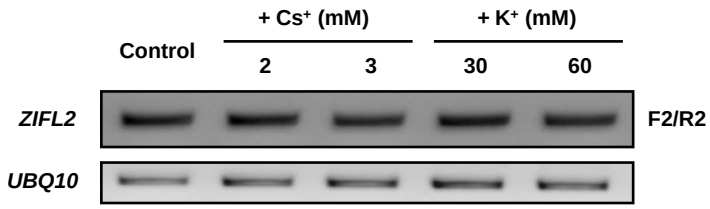

Fig. S4 RT-PCR analysis of *ZIFL2* expression in 7-d old wild-type (Col-0) seedlings grown under control conditions (~20 mM K^+) or challenged for 48h with various Cs^+ or K^+ supplies. The location of the F2 and R2 primers used is shown in Figure 1A. Expression of the *UBQ10* gene is shown as a loading control. Results are representative of two independent experiments.

Table S1 Sequences of the primers used in this study.

PRIMER NAME	SEQUENCE (5' to 3')
Expression analyses	
F1	TCATCAACCAGTCCGA
F2	GTCTATGCTACTGCGGTTCTC
F3	CCCGCCATTGGAGAA
F4	GGTGTTGAATTTGGTACAGC
R1	AAGCAGCCAAGAAGAAA
R2	GAAACACCAGAAGCCCAAG
R3	TCATCACATGGTGCAAAAA
R4	CCGAATCATAGAGAAACACA
R4'	CGTGCGTCGTGACAACT
ROC1-F	GTCTGATAGAGATCTCACGT
ROC1-R	AATCGGCAACAACAACAGGC
UBQ10-F1	GATCTTTGCCGGAAAACAATTGG
UBQ10-R1	TAGAAAGAAAGAGATAACAGG
Cloning of Pro*ZIFL2:GUS-GFP* construct	
ProZIFL2-F	TT*GAGCTC*AACTGTAAAATCGTCGTGAA
ProZIFL2-R	TT*CCGCGG*GATCGGAACCACTGAGTC
Cloning of Pro*35S:ZIFL2.1-YFP* and Pro*35S*:*ZIFL2.1-GFP* constructs	
ZIF2YFP-F	TT*CTCGAG*TTGGAATGAAATAAAAAT
ZIF2YFP-R	TT*AATTAA*CTGGATTTGGGAAATGT

Restriction sites are shown in italics and underlined.